

# Nonlocal discrete continuity and invariant currents in locally symmetric effective Schrödinger arrays

C. V. Morfonios,<sup>1</sup> P. A. Kalozoumis,<sup>2</sup> F. K. Diakonou,<sup>2</sup> and P. Schmelcher<sup>1,3</sup>

<sup>1</sup>*Zentrum für Optische Quantentechnologien, Universität Hamburg, 22761 Hamburg, Germany*

<sup>2</sup>*Department of Physics, University of Athens, 15771 Athens, Greece*

<sup>3</sup>*The Hamburg Centre for Ultrafast Imaging, Universität Hamburg, 22761 Hamburg, Germany*

(Dated: April 26, 2022)

A nonlocal discrete continuity formalism is developed which relates spatial symmetries in subparts of Hermitian or non-Hermitian lattice systems to the properties of adapted nonlocal currents. Broken local symmetries thereby act as current sources or sinks, and the time evolution of the associated nonlocal charge is governed by the nonlocal currents at the boundaries of domains with local symmetry. We apply the framework to locally inversion-(time-) and translation-(time-) symmetric one-dimensional photonic waveguide arrays effectively described by Schrödinger's equation with a tight-binding Hamiltonian. The nonlocal currents of stationary states are shown to be translationally invariant within local symmetry domains for arbitrary wavefunction profiles, and cases of complete, overlapping, and gapped local symmetry are demonstrated for model setups. Two distinct versions of the nonlocal invariant currents enable a mapping between wave amplitudes of symmetry-related sites, thereby generalizing the global Bloch and parity mapping to local translation and inversion symmetry in discrete systems. In scattering setups, perfectly transmitting states are characterized by aligned nonlocal invariants in attached symmetry domains, whose vanishing signifies a correspondingly symmetric density. For periodically driven arrays, the invariance of the nonlocal currents is retained on period average for quasi-energy eigenstates. Encoding local potential and coupling symmetries into arbitrary stationary states, the theory of symmetry-induced continuity and local invariants may contribute to the understanding of wave structure and response in systems with localized spatial order.

PACS numbers: 03.65.-w, 42.25.Bs, 42.82.Et, 78.67.Pt

## I. INTRODUCTION

Symmetry under spatial transformations is a simple yet fundamental concept underlying the description of most systems in contemporary physics as the origin of conserved quantities. In quantum theory and wave mechanics, symmetry-induced conservation laws are extended from continuous to discrete transformations in terms of commutation of the corresponding operators with the Hamiltonian, which in turn dictates the spatial structure of stationary states. Ubiquitous paradigms are reflection ( $\mathcal{P}$ ) or finite translation ( $\mathcal{K}$ ) symmetry imposing definite parity or Bloch momentum on Hamiltonian eigenstates, which then provide the basis for understanding phenomena such as selection rules of level transitions in atoms [1] or the formation of band structure in crystals [2]. In intricate lattice systems of intense current interest such as topological insulators [3], Weyl semimetals [4], and Lieb lattices [5], state localization and transport properties are also predominantly traced back to broken or unbroken spatial symmetries in combination with the operation of time reversal ( $\mathcal{T}$ ). The significance of broken spatiotemporal symmetries and has further been addressed for driven quantum systems [6, 7] in relation to directional transport [8].

Since symmetries are naturally addressed with respect to commutation with the global system Hamiltonian, they are usually regarded dichotomously as broken or unbroken. Nevertheless, in a composite system the Hamiltonian elements may retain a certain spatial symmetry *locally* in a subdomain of configuration space although it is broken *globally*; we refer to this case as a 'local symmetry' (LS). Although there is clearly a remnant of the considered symmetry in the corresponding subsystem, it is not evident how to track this information in the eigenstates of the Hamiltonian since it generally does not commute with the LS operation. At the same time, LSs are actually inherently paramount to a variety of systems such as aperiodic lattices with long-range order [9–12], partially disordered media [13–15], and single complex molecules [16, 17]. A typical example are also generic solid

state nanostructures [18] where unavoidable impurities and defects (usually modeled as  $\mathcal{P}$ -symmetric) separate the host crystal into finite  $\mathcal{K}$ -symmetric parts. LS may also be present by design in artificial devices like, e. g., multilayered photonic setups [19, 20], acoustic waveguides [21, 22], or magnonic systems [23], due to restrictions of finiteness or functionality. In fact, even global spatial symmetry is generally rendered local as soon as a system's immediate environment is included in the description.

The spatial structure of stationary states in continuous, one-dimensional (1D), locally symmetric scattering potentials was recently pinpointed within the framework of symmetry-adapted nonlocal currents (NLCs) [24–26]: At any real frequency, two distinct NLCs are spatially constant within subdomains of local  $\mathcal{P}$  or  $\mathcal{K}$  symmetry. They provide a mapping of field amplitudes between LS related points, thus generalizing the mapping through parity or Bloch factors for global symmetry [25]. The NLCs were further linked to perfectly transmitting states [27] and proposed as a natural order parameter for spontaneous symmetry breaking in non-Hermitian  $\mathcal{PT}$ -symmetric systems [28, 29], as well as observed experimentally in lossy acoustic setups [30].

The stationary translational invariance of the NLCs suggests that they are governed by a continuity equation incorporating the associated symmetry transform. In the case of global space reflection  $\mathcal{P}$ , a continuous two-point version of the quantum current density is intricately related to the combination of  $\mathcal{P}$  with the operation of time reversal  $\mathcal{T}$  [31, 32]. A similar bilocal picture of quantum mechanics has also been used in an alternative description of double slit interference [33]. Conservation of the two-point current in 1D continuous  $\mathcal{PT}$ -symmetric systems can be derived from Schrödinger's [31, 32, 34], or via gauge invariance of a nonlocal Lagrangian [35] in analogy to local current conservation. Global  $\mathcal{PT}$  symmetry has gained increased attention since it admits real discrete spectrum for non-Hermitian systems [36] in parametric regions where density loss and gain are balanced [37], and has been intensively investigated in wave scattering [34, 38–41].

Non-Hermitian Hamiltonians are of particular interest in discrete models, where the coupling between sites constitutes an additional degree of freedom for design and control [42]. A reliable platform of applicability is provided by photonic waveguide arrays which are well described by an effective discrete Schrödinger equation with tight-binding Hamiltonian [34, 43]. Discrete arrays are ideal for implementing global or local spatial symmetries, by adjusting the onsite Hamiltonian elements or the inter-site hoppings, to study their impact on field state properties. As an example, in a certain class of discrete structures with ‘hidden’ symmetries in the state space [44], conserved quantities from global operators commuting with the Hamiltonian can be identified. Partial  $\mathcal{PT}$  symmetry along a given coordinate has also been implemented in the form of dimer arrays featuring synchronous Bloch-Zener oscillations [45] or synthetic lattices with solitonic excitations [46]. In discrete models, even the local current becomes a two-point quantity, naturally defined to flow on the ‘link’ between two lattice sites [47, 48]. This raises the question of how to formulate discrete conservation laws for nonlocal quantities entailing different links. In view of LS, such a framework would provide the relation between nonlocal link currents to general lattice symmetry transformations restricted to subdomains of a composite system.

In the present work, we combine the concept of local symmetry transformations with that of nonlocal current continuity for discrete—generally non-Hermitian—Schrödinger models. We thereby identify the breaking of LSs as sources for the NLCs flowing along transformation related links. The NLCs are given in operator form, thus making the extension to multiple links per site straightforward. With photonic waveguide arrays in mind, we apply the framework to 1D tight-binding Hermitian and non-Hermitian lattice systems with local  $\mathcal{S}$  or  $\mathcal{ST}$  symmetry, respectively, with  $\mathcal{S} = \mathcal{P}$  (inversion) or  $\mathcal{K}$  (finite translation). The evolution of the associated nonlocal charge is given in terms of the NLCs at the boundaries of locally symmetric domains, based on a symmetry-induced discrete Gauss law. Together with an alternatively defined NLC, identities are derived which relate the amplitudes of general states at symmetry-transformed sites and connect the NLCs with the local current. For stationary states, the LSs thereby induce amplitude mappings within finite domains. The domainwise translation invariance of the NLCs in stationary states is demonstrated for different types of LS, including their generalized analogue for periodically modulated arrays. It is thus demonstrated how the NLCs reveal the Hamiltonian LSs encoded in arbitrarily irregular eigenstates. Finally, the density profile of perfectly transmitting scattering states is shown to be characterized by NLCs in terms of its LS.

The paper is organized as follows. In Sec. II we introduce the concept of LSs in terms of the corresponding local permutation matrices and nonlocal site projection operators. Section III is devoted to the discrete nonlocal continuity and the relation of the NLCs and associated nonlocal charge to LSs. In Sec. IV we address the properties of NLCs in stationary states, derive the symmetry-induced amplitude mapping relations and the connection to the local current, and generalize the NLC to driven arrays. In Sec. V we discuss the cases of complete, overlapping, and gapped LS, and provide examples of invariant NLCs in non-Hermitian and driven finite arrays. In section Sec. VI we consider the NLCs in scattering states, derive their relation to perfect transmission and illustrate their invariance in locally symmetric non-Hermitian scatterers. Section VII concludes the paper and provides perspectives for generalizations and future work.

## II. LOCAL SYMMETRY OPERATIONS

To define the concept and explicit form of a LS operation in a 1D discrete model, we start by considering a single-particle, time-independent Hamiltonian  $\hat{H}$  represented on  $N$  localized site excitations  $|n\rangle$ ,  $n = 1, 2, \dots, N$ , with onsite potential elements  $v_n = H_{nn} = \langle n|\hat{H}|n\rangle$  and hopping elements  $h_{n,n'} = H_{nn'} = \langle n|\hat{H}|n'\rangle$  from site  $n'$  to  $n \neq n'$ . The temporal evolution of a quantum state

$$|\psi\rangle = \sum_{n=1}^N \psi_n |n\rangle \quad (1)$$

is then governed by the Schrödinger equation (SE)

$$i\partial_t |\psi\rangle = \hat{H} |\psi\rangle \quad (2)$$

where we set  $\hbar = 1$ . Such a discrete model is widely used to describe coherent electron transport in 1D lattice potentials like the ones induced in quantum dot arrays, but also as a finite difference approximation to the continuous SE by choosing appropriate (typically equal) hopping values. In particular, Eq. (2) effectively also describes light propagation in photonic waveguide arrays within the paraxial approximation [34, 43] for small lateral wave vector components. 1D versions of such a photonic array are schematically depicted in Fig. 1. Time  $t$  is here represented by the longitudinal spatial coordinate  $z$  along the waveguides, and energy  $E$  is accordingly represented by the light propagation constant along  $z$ . Onsite potentials  $v_n$  correspond to the refractive indices of waveguides, while the hoppings  $h_{n,n'}$  are proportional to the overlap of the light field localized in waveguides  $n, n'$  and thereby mapped to their distance. Remarkable agreement with experimental results is achieved already in the tight-binding approximation [49] with  $h_{n,n'} = 0$  for  $|n - n'| > 1$ , which we will focus on in the following.

Given the above framework for a discrete 1D Schrödinger model, we consider a bijective mapping  $\mathcal{S}_{\mathbb{D}} : \mathbb{D} \rightarrow \mathbb{D}$  given by

$$\mathcal{S}_{\mathbb{D}} : n \rightarrow \bar{n} = \mathcal{S}_{\mathbb{D}}(n) = \begin{cases} \mathcal{P}_{\mathbb{D}}(n) & = 2\alpha - n \\ \mathcal{K}_{\mathbb{D}}(n) & = L + n \end{cases}, \quad (3)$$

which performs a local inversion ( $\mathcal{P}$ ) through a center  $\alpha$  or translation ( $\mathcal{K}$ ) by a length  $L$  of sites  $n \in \mathbb{D}$  to sites  $\bar{n} \in \mathbb{D}$ , where the domain  $\mathbb{D} \subseteq \mathbb{N}$  is generally a subset of the total set  $\mathbb{N}$  of all sites. Suppose now that the discrete system described by the Hamiltonian elements  $H_{mn}$  remains invariant under this site mapping, that is,

$$H_{\bar{m}\bar{n}} = H_{mn} \quad \forall m, n \in \mathbb{D}, \quad (4)$$

so that  $\mathcal{S}_{\mathbb{D}}$  is a symmetry transformation of the system. We then say that the system possesses a *local* symmetry in the union  $\mathbb{U} \equiv \mathbb{D} \cup \mathbb{D}$ . A LS is thus contrasted with a *global* symmetry of the system for which  $\mathbb{D} = \mathbb{N}$ . Locally  $\mathcal{P}$ - and  $\mathcal{K}$ -symmetric photonic arrays are depicted in Fig. 1 (a) and (b), respectively. The discrete parameters  $\alpha$  and  $L$  here refer to the site indexing and not to the continuous coordinate along the array: The center  $\alpha$  is integer (half integer) for odd (even) number of sites  $D$  in  $\mathbb{D}$ , and the integer period  $L$  is the shift in site number to the right. Intersite distances in the physical system are mapped to corresponding hopping element magnitudes in the model, determined by evanescent field overlap between waveguides in photonics [49]. Thus, a local inversion

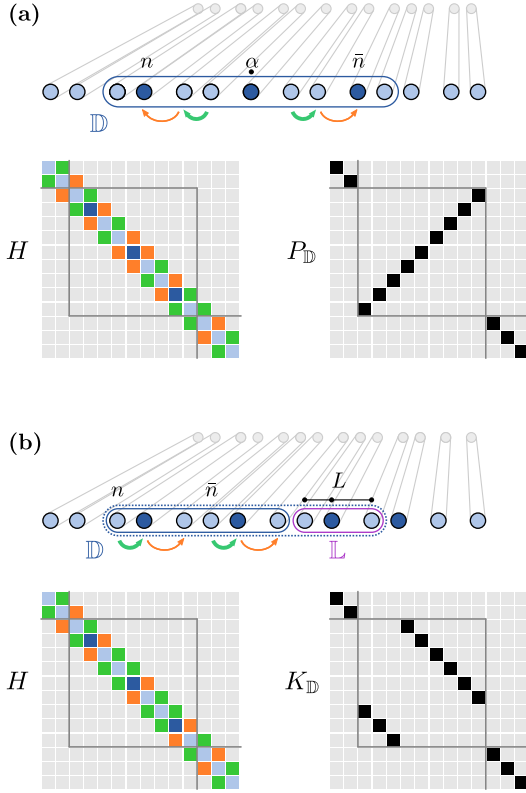


FIG. 1. Sketch of a 1D finite lattice in the form of a photonic waveguide array which is (a) locally inversion ( $\mathcal{P}$ ) symmetric about a center  $\alpha$  or (b) translation ( $\mathcal{K}$ ) symmetric with period  $L$ , for sites  $n$  within a domain  $\mathbb{D}$  (solid blue line), together with the corresponding close-coupling Hamiltonian matrix  $H$  and local transformation (site permutation) matrix  $P_{\mathbb{D}}$  or  $K_{\mathbb{D}}$ , respectively.  $P_{\mathbb{D}}$  maps  $\mathbb{D}$  to itself, while  $K_{\mathbb{D}}$  performs a cyclic shift permutation by  $L$  sites on  $\mathbb{U} = \mathbb{D} \cup \mathbb{L}$ , where  $\mathbb{L}$  (solid purple line) is the rightmost period in  $\mathbb{U}$  (dotted blue line).

maps a domain  $\mathbb{D}$  to itself, so that  $\mathbb{D} = \bar{\mathbb{D}} = \mathbb{U}$ , while a local translation shifts  $\mathbb{D}$  by  $L$  sites, so that  $\mathbb{U} = \mathbb{D} \cup \mathbb{L}$  where  $\mathbb{L}$  are the rightmost  $L$  sites in  $\mathbb{U}$  (see Fig. 1) for  $L \leq D$  (the case  $L > D$  will be treated later in Sec. V A).

With the (symmetry) mapping  $\mathcal{S}_{\mathbb{D}}$  transforming the site indices  $n$ , we correspondingly define an operator

$$\hat{\Sigma} = \sum_{n=1}^N \hat{\sigma}_n, \quad \hat{\sigma}_n = |n\rangle \langle \mathcal{S}_{\mathbb{D}}(n)| = |n\rangle \langle \bar{n}| \quad (5)$$

which replaces the wave amplitude  $\psi_n$  with  $\psi_{\bar{n}}$  for the basis ket  $|n\rangle$  when acting on a state  $|\psi\rangle$  (cf. Eq. (1)),

$$\hat{\Sigma} |\psi\rangle = \sum_{n=1}^N \psi_{\bar{n}} |n\rangle \equiv |\bar{\psi}\rangle, \quad (6)$$

since the basis  $\{|n\rangle\}$  is assumed orthonormal ( $\langle m|n\rangle = \delta_{mn}$ ), so that we can symbolically write the action as an amplitude mapping

$$\hat{\Sigma}_{\mathbb{D}} : \psi_n \rightarrow \psi_{\bar{n}}, \quad \hat{\Sigma}_{\mathbb{D}} = \hat{P}_{\mathbb{D}}, \hat{K}_{\mathbb{D}}, \quad (7)$$

in analogy with the local *site* mapping in Eq. (3) for  $\mathcal{S}_{\mathbb{D}} = \mathcal{P}_{\mathbb{D}}, \mathcal{K}_{\mathbb{D}}$ . The associated matrix  $\Sigma_{\mathbb{D}}$  has elements  $[\Sigma_{\mathbb{D}}]_{mn} = \langle m|\hat{\Sigma}|n\rangle$  given by

$$[\Sigma_{\mathbb{D}}]_{mn} = \begin{cases} \delta_{\bar{m}n}, & m \in \mathbb{D} \\ \delta_{mn}, & m \in \mathbb{N} \setminus \mathbb{U} \end{cases}, \quad \Sigma_{\mathbb{D}} = P_{\mathbb{D}}, K_{\mathbb{D}}. \quad (8)$$

For local inversion,  $P_{\mathbb{D}}$  performs a (partial) mirror permutation of the sites within  $\mathbb{D}$ . For local translation, Eq. (8) leaves the mapping of sites  $m \in \mathbb{L}$  undefined, for which we explicitly choose  $[\Sigma_{\mathbb{D}}]_{mn} = \delta_{\bar{m}-D,n}$  so that the last  $L$  sites in  $\mathbb{U}$  are mapped to the first  $L$  ones. The permutation matrix thus acts on the whole array but permutes only sites amplitudes within the domain  $\mathbb{U}$  where the LS of the system resides while leaving sites outside  $\mathbb{U}$  unchanged. Note that multiple symmetry domains  $\mathbb{D}_d$  ( $d = 1, 2, \dots$ ) may in general be present, with corresponding centers  $\alpha_d$  or periods  $L_d$ . The total symmetry domain is then the (generally disconnected) set  $\mathbb{D} = \bigcup_d \mathbb{D}_d$ , with the mapping for each separate  $\mathbb{D}_d$  entering Eq. (8). Different types of LS will be addressed in Sec. V A.

Symmetry of a system under a transformation is usually associated with the commutation of the corresponding symmetry operator with the Hamiltonian. In the case of global symmetry, that is,  $\mathbb{D} = \mathbb{N}$  in the present setting (with  $N = \infty$  implied for translation symmetry), the Hamiltonian indeed commutes with the matrix  $\Sigma_{\mathbb{D}}$  and the energy eigenstates are also eigenstates of the symmetry operation with the corresponding eigenvalues: Under inversion or translation the wave amplitudes are mapped to  $\psi_{\bar{n}} = \lambda \psi_n$  with the parity  $\lambda = \pm 1$  or the Bloch phase  $\lambda = e^{ikL}$  ( $k$  being the quasimomentum) as prefactors, respectively. In the case of a LS, although the system remains invariant under the site permutation, the associated operator generally does not commute with the Hamiltonian,

$$[\hat{\Sigma}_{\mathbb{D}}, \hat{H}] \neq 0. \quad (9)$$

The reason is the change in connectivity of the domain  $\mathbb{D}$  to its surroundings: The end sites of  $\mathbb{D}$  in a 1D array are not coupled to the same sites after the local permutation, and so the transformed Hamiltonian  $\bar{H} \equiv \Sigma^\dagger H \Sigma$  (recall that  $\Sigma^{-1} = \Sigma^\dagger$  for any permutation matrix) generally contains altered nonzero hopping elements  $\bar{H}_{mn} \neq H_{mn}$  for  $m \in \mathbb{D}$  and  $n \notin \mathbb{D}$ ; cf. Eq. (4).

The spatial structure of system eigenstates is therefore no longer dictated directly by the presence of symmetry as in the global case where the field magnitude  $|\psi_n|^2$  has the  $\Sigma$ -symmetry of the potential. The inequivalence between *system* symmetry and commutation of the symmetry operation with the Hamiltonian does not come as a surprise: A trivial example is a finite homogeneous tight-binding array (with  $v_n = v, h_{n,n\pm 1} = h \forall n$ ) which is obviously invariant under *any* arbitrary site permutation whose matrix, however, does not commute with  $H$  (except for mirror permutation), since it changes the intersite connections, as explained above. The question raised here is, nevertheless, if the presence of symmetries in the system are in some way imprinted on the structure of its states, even if those symmetries are not global but of finite extent. The aim is thus to find a characterization of the field amplitude configuration in terms of a quantity which follows the underlying LSs of the system. To do so, in the following section we turn to the notion of nonlocal current-density continuity in its discrete form and adapt it to the LS framework.

Before closing this section, we need to extend the defined local spatial transformations to their combination with the operation of time-reversal  $\mathcal{T} : t \rightarrow -t$ , represented here as usual by an antiunitary operator  $\hat{T} = \hat{T}^{-1}$  performing complex conjugation [50],

$$\hat{T} : i \rightarrow -i; \quad \hat{T} i \hat{T} = -i, \quad (10)$$

in the spatial representation. Time-reversal thus acts on a state

in the basis  $\{|n\rangle\}$  as

$$\hat{T}|\psi\rangle(t) = \sum_n \psi_n^*(-t)|n\rangle \equiv |\psi^\tau\rangle \quad (11)$$

and transforms the Hamiltonian as  $\hat{T}\hat{H}\hat{T} = \hat{H}^*$  (defined by  $\langle m|\hat{H}^*|n\rangle = H_{mn}^*$ ). The latter becomes relevant for complex onsite elements

$$v_n \equiv u_n + i\frac{\gamma_n}{2} \quad (u_n, \gamma_n \in \mathbb{R}), \quad (12)$$

where positive (negative)  $\gamma_n$  models the gain (loss) rate of the state density at site  $n$  (as clarified in the next section), while complex hoppings  $h_{n,n'} = |h_{n,n'}|e^{i\varphi_{n,n'}}$  with Peierls phase  $\varphi_{n,n'}$  generally arise from the presence of gauge fields (effectively also in 1D systems [51]). If the Hamiltonian obeys (cf. Eq.(4))

$$H_{\bar{m}\bar{n}} = H_{mn}^* \quad \forall m, n \in \mathbb{D}, \quad (13)$$

then we will call the system locally  $\mathcal{ST}$ -symmetric, that is,  $\mathcal{PT}$ -symmetric or  $\mathcal{KT}$ -symmetric within the finite spatial domain  $\mathbb{U} = \mathbb{D} \cup \bar{\mathbb{D}}$ . Note here that we treat (local) non-Hermiticity, expressed through the  $\gamma_n$ , solely as an *effective* simple model to express gain or loss of density from or to the surrounding medium, rather than a fundamental description of the physical system.

### III. DISCRETE NONLOCAL CURRENT-DENSITY CONTINUITY

Having defined the concept of LS for lattice systems, we shall now generalize the discrete continuity relation [48] to a nonlocal form adapted to a given the symmetry mapping.

#### A. Local continuity

In equivalence to the Schrödinger equation (2) for a general state  $|\psi\rangle$ , the temporal evolution of the local density  $\rho_n = \langle\psi|\hat{\rho}_n|\psi\rangle = \psi_n^*\psi_n$  fulfills the discrete continuity equation

$$\partial_t \rho_n = j_n - i(v_n - v_n^*)\rho_n = j_n + \gamma_n \rho_n, \quad (14)$$

with  $\hat{\rho}_n \equiv |n\rangle\langle n|$  being the local density operator in the Schrödinger picture, where  $j_n = j_n^+ + j_n^-$  is the sum of the magnitudes

$$\begin{aligned} j_n^\pm &\equiv j_{n,n\pm 1} \\ &= \frac{1}{i} (\psi_n^* h_{n,n\pm 1} \psi_{n\pm 1} - \psi_{n\pm 1}^* h_{n,n\pm 1}^* \psi_n) \end{aligned} \quad (15)$$

of the currents  $j_n^\pm$  flowing inwards from sites  $n \pm 1$  to site  $n$ . Under the assumption of Hermitian hoppings,  $h_{n,n\pm 1}^* = h_{n\pm 1,n}$ , the total current magnitude can be written as the expectation value  $j_n = \langle\psi|\hat{j}_n|\psi\rangle$  of a current operator

$$\hat{j}_n = \hat{j}_n^+ + \hat{j}_n^- = \frac{1}{i} [\hat{\rho}_n, \hat{H}] \quad (16)$$

assigned to site  $n$ . Note that the discrete form of the current divergence entering the continuity equation is generally given by the sum of the projections  $j_{nm} = \mathbf{j}_{nm} \cdot \mathbf{e}_{nm}$  of the link currents  $\mathbf{j}_{nm}$  from point  $\mathbf{r}_m$  to point  $\mathbf{r}_n$  onto their directions  $\mathbf{e}_{nm}$ , scaled by the distance  $|\mathbf{r}_n - \mathbf{r}_m|$  [48]. The local

(referring to site  $n$ ) continuity equation (14) shows that the imaginary part  $2\gamma_n$  of the onsite element  $v_n$  acts like a source ( $\gamma_n > 0$ ) or sink ( $\gamma_n < 0$ ) of density  $\rho_n$  at site  $n$ , in addition to the inflow of current  $j_n$ . The partial link current operators producing the  $j_n^\pm$  can be written as [47]  $\hat{j}_n^\pm = \hat{\rho}_n \hat{v}^\pm + \hat{v}^\mp \hat{\rho}_n$  in terms of the parital velocity operators  $\hat{v}^\pm = \frac{1}{i} [\hat{r}, \hat{H}^\pm]$  with  $\hat{r} = \sum_n \mathbf{r}_n \hat{\rho}_n$  being the position operator, such that the operators producing the projections  $j_n^\pm$  are given by

$$\hat{j}_n^\pm = \frac{1}{i} (\hat{\rho}_n \hat{H}^\pm - \hat{H}^\mp \hat{\rho}_n). \quad (17)$$

Here, the  $\hat{H}^\pm$  are the ‘hopping operators’ with matrix elements  $\langle n|\hat{H}^\pm|m\rangle = h_{n,m} \delta_{n\pm 1,m}$ , that is, the upper/lower diagonal of the tridiagonal matrix  $H$  in the tight-binding case.

#### B. Nonlocal continuity

With respect to the spatial transformation  $\mathcal{S}_\mathbb{D}$ , we now generalize the local discrete continuity equation in Eq. (14) to a nonlocal form by replacing the  $\hat{\rho}_n$  with  $\hat{\sigma}_n = |n\rangle\langle \bar{n}|$  from Eq. (5). The latter is now identified with a nonlocal density operator corresponding to the off-diagonal part of the site-represented density operator  $\hat{\rho} = |\psi\rangle\langle\psi|$  associated with the transformation  $\mathcal{S}$ , so that

$$\sigma_n \equiv \langle\psi|\hat{\sigma}_n|\psi\rangle = \langle\bar{n}|\hat{\rho}|n\rangle = \psi_n^* \psi_{\bar{n}}, \quad (18)$$

constitutes a symmetry-adapted nonlocal density in state  $\psi$ , while its sum over  $n$  yields the total ‘nonlocal charge’

$$\Sigma_\psi = \langle\psi|\hat{\Sigma}|\psi\rangle = \sum_n \sigma_n, \quad (19)$$

also known as ‘quasipower’ [52] in globally  $\mathcal{PT}$ -symmetric photonic systems, in analogy to the usual charge (i. e. quantum probability), or power in photonics,  $I_\psi = \langle\psi|\hat{I}|\psi\rangle = \sum_n \rho_n$  ( $\hat{I}$  being the identity operator). Using the SE, the temporal evolution of  $\sigma_n$  is given by

$$\partial_t \sigma_n = q_n - i(v_n - v_n^*)\sigma_n = q_n + \beta_n \sigma_n, \quad (20)$$

with  $\beta_n \equiv (v_n - v_n^*)/i$  characterizing the onsite asymmetry, and where  $q_n = q_n^+ + q_n^-$  assigned to site  $n$  is the sum of the *nonlocal* currents defined by

$$\begin{aligned} i q_n^\pm &\equiv i q_{n,\mathcal{S}}^\pm \equiv i q_{n,n\pm 1;\mathcal{S}} = \\ &\psi_n^* h_{\mathcal{S}(n),\mathcal{S}(n\pm 1)} \psi_{\mathcal{S}(n\pm 1)} - \psi_{n\pm 1}^* h_{n,n\pm 1}^* \psi_{\mathcal{S}(n)} \end{aligned} \quad (21)$$

for a local transformation  $\mathcal{S} = \mathcal{S}_\mathbb{D}$  given in Eq.(3), with  $\mathcal{S}(n \pm 1) = \bar{n} \mp 1$  and  $\bar{n} \pm 1$  for  $\mathcal{S} = \mathcal{P}$  (inversion) and  $\mathcal{K}$  (translation), respectively. Considering Hermitian hoppings,  $\hat{H}^\mp = [\hat{H}^\pm]^\dagger$ , these four-site currents  $q_{n,\mathcal{P}}^\pm$  and  $q_{n,\mathcal{K}}^\pm$  can be written as the expectation values

$$q_{n,\mathcal{S}}^\pm = \langle\psi|\hat{q}_{n,\mathcal{S}}^\pm|\psi\rangle \quad (\mathcal{S} = \mathcal{P}, \mathcal{K}) \quad (22)$$

of the corresponding nonlocal current operators

$$\hat{q}_{n,\mathcal{P}}^\pm = \frac{1}{i} (\hat{\sigma}_{n,\mathcal{P}} \hat{H}^\pm - \hat{H}^\pm \hat{\sigma}_{n,\mathcal{P}}), \quad (23)$$

$$\hat{q}_{n,\mathcal{K}}^\pm = \frac{1}{i} (\hat{\sigma}_{n,\mathcal{K}} \hat{H}^\pm - \hat{H}^\mp \hat{\sigma}_{n,\mathcal{K}}), \quad (24)$$

in analogy with Eq.(17), with the transformation type  $\mathcal{P}$  or  $\mathcal{K}$  entering  $\hat{\sigma}$  here explicitly indicated. Outside the domain  $\mathbb{U}$  of

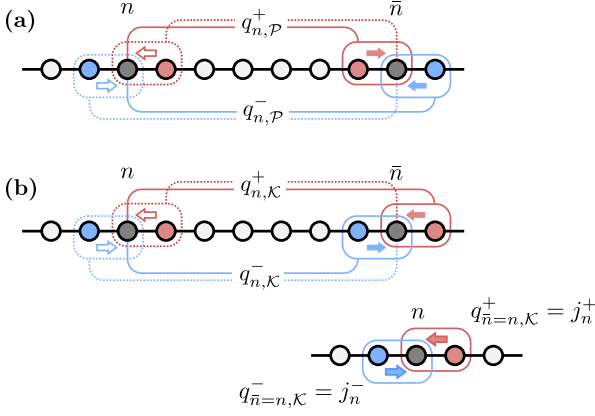


FIG. 2. Nonlocal current flow on pairs of  $\mathcal{S}$ -related links for (a) inversion  $\mathcal{S} = \mathcal{P}$  and (b) translation  $\mathcal{S} = \mathcal{K}$  transform. Solid (dotted) lines indicate the term  $\psi_n^* h_{\mathcal{S}(n), \mathcal{S}(n\pm 1)} \psi_{\mathcal{S}(n\pm 1)}$  ( $\psi_{n\pm 1}^* h_{n, n\pm 1}^* \psi_{\mathcal{S}(n)}$ ) entering each upper (+) and lower (-) NLC  $q_{n, \mathcal{S}}^\pm$  ( $\mathcal{S} = \mathcal{P}, \mathcal{K}$ ) on the links into a site pair  $n, \bar{n}$ ; see Eq.(21). Inset: The translation NLC reproduces the local link current  $j_n^\pm$  for  $\bar{n} = n$ .

the mapping where  $\bar{n} = n$ , the translation current reproduces the usual current,  $\hat{q}_{\bar{n}=n, \mathcal{K}}^\pm = \hat{j}_n^\pm$ , and so Eq. (20) reproduces the local current-density continuity in Eq. (14). For both  $\mathcal{P}$  and  $\mathcal{K}$ , the total current operator is given by

$$\hat{q}_n = \hat{q}_n^+ + \hat{q}_n^- = \frac{1}{i} [\hat{\sigma}_n, \hat{H} - \hat{V}], \quad (25)$$

where  $\hat{V} = \hat{H} - \hat{H}^+ - \hat{H}^-$  is the diagonal part of the Hamiltonian. Note here that, like the usual currents  $j_n^\pm$ , the  $q_n^\pm$  can be seen as link currents, though not flowing along one link but along the two ones corresponding to the hoppings  $h_{\mathcal{S}(n), \mathcal{S}(n\pm 1)}$  and  $h_{n, n\pm 1}^*$  entering Eq. (21). This nonlocal ‘flow’ is illustrated in Fig. 2.

Using the transformation matrices  $\Sigma_{\mathbb{D}} = P_{\mathbb{D}}, K_{\mathbb{D}}$  defined in Eq. (8) (and depicted in the example of Fig. 1), the  $q_n^\pm = \langle \psi | \hat{q}_n^\pm | \psi \rangle$  in Eq. (21) for the whole setup  $\mathbb{N}$  can be written as the components of an  $N$ -entry column vector  $\mathbf{q}^\pm = [q_1^\pm, q_2^\pm, \dots, q_N^\pm]^\top$  given by (cf. Eqs.(23) and (24))

$$i\mathbf{q}_{\mathcal{P}}^\pm = \mathbf{d}[\psi^\dagger] P_{\mathbb{D}} H^\pm \psi - \mathbf{d}[\psi^\dagger H^\pm] P_{\mathbb{D}} \psi, \quad (26a)$$

$$i\mathbf{q}_{\mathcal{K}}^\pm = \mathbf{d}[\psi^\dagger] K_{\mathbb{D}} H^\pm \psi - \mathbf{d}[\psi^\dagger H^\mp] K_{\mathbb{D}} \psi \quad (26b)$$

for local  $\mathcal{P}, \mathcal{K}$ -transformation, respectively, where  $\psi = [\psi_1, \psi_2, \dots, \psi_N]^\top$  and  $\mathbf{d}[\mathbf{a}]$  denotes the  $N \times N$  diagonal matrix with the components of (row or column) vector  $\mathbf{a}$  along its diagonal. Recall here the convention of mapping the last period  $\mathbb{L}$  of a domain  $\mathbb{U}$  to the first one for  $\mathcal{K}$ -transforms. The above expression for the  $q_n^\pm$  becomes convenient when evaluating them for a given Hamiltonian and (numerically computed) state amplitudes  $\psi_n$ , as will be done in the following sections.

For a given site transformation  $\mathcal{S}$ , the form of the nonlocal continuity equation (20) is similar to Eq. (14) with the loss/gain function  $\gamma_n$  replaced by  $\beta_n$  which characterizes the sources for the nonlocal density  $\sigma_n$ . For a system with  $\mathcal{S}$ -symmetric onsite potential,  $v_{\bar{n}} = v_n$  or  $[\hat{V}, \hat{\Sigma}] = 0$ , we have  $\beta_n = \gamma_n$  and the sources (sinks) of  $\sigma_n$  are represented by the gain (loss) of  $\rho_n$  at individual sites  $n$  like in Eq. (14), and  $\hat{q}_n = [\hat{\sigma}_n, \hat{H}]/i$  like in Eq. (16). Those sources and sinks vanish if the potential is real, but if the  $v_n$  are not  $\mathcal{S}$ -symmetric, then in Eq. (20) there is a contribution to  $\beta_n$  from the potential differences between  $\mathcal{S}$ -related sites. In other words,

locally *broken spatial potential symmetries act as sources* for the associated nonlocal density. If a system has locally  $\mathcal{ST}$ -symmetric non-Hermitian onsite potential,  $v_{\bar{n}} = v_n^*$  or  $[\hat{V}, \hat{\Sigma}\hat{T}] = 0$ , then  $\beta_n = 0$  within the symmetry domain  $\mathbb{D}$  and Eq. (20) reduces to  $\partial_t \sigma_n = q_n$ . This means that the net NLC  $q_n$  vanishes within  $\mathbb{D}$  for stationary states, in contrast to  $j_n$  which may vary spatially for  $\gamma_n \neq 0$ ; see Eq. (14).

An alternative nonlocal continuity equation can finally be established by projecting  $\hat{\sigma} |\psi\rangle$  onto the time-reversed state  $\mathcal{T} |\psi\rangle = |\psi^\tau\rangle$  instead of  $|\psi\rangle$  in Eq. (18), yielding a *bitemporal* nonlocal ‘density’

$$\sigma_n^\tau \equiv \langle \psi^\tau | \hat{\sigma}_n | \psi \rangle = \psi_n(-t) \psi_{\bar{n}}(t). \quad (27)$$

Using the SE, the evolution of  $\sigma_n^\tau$  can be shown to obey the continuity equation

$$\partial_t \sigma_n^\tau = q_n^\tau - i(v_{\bar{n}} - v_n) \sigma_n^\tau = q_n^\tau + \xi_n \sigma_n^\tau, \quad (28)$$

now with asymmetry function  $\xi_n \equiv (v_{\bar{n}} - v_n)/i$  and with bitemporal net NLC  $q_n^\tau = q_n^{\tau+} + q_n^{\tau-}$  flowing into site  $n$ , where

$$iq_n^{\tau\pm} \equiv iq_{n, \mathcal{S}}^{\tau\pm} \equiv iq_{n, n\pm 1; \mathcal{S}}^\tau = \quad (29)$$

$$\psi_n(-t) h_{\mathcal{S}(n), \mathcal{S}(n\pm 1)} \psi_{\mathcal{S}(n\pm 1)}(t) - \psi_{n\pm 1}(-t) h_{n, n\pm 1} \psi_{\mathcal{S}(n)}(t),$$

defined in similarity to the NLCs in Eq. (21). Under the assumption of *equidirectional* hoppings, so that  $\hat{H}^\mp = [\hat{H}^\mp]^\top$ , the  $q_{n, \mathcal{S}}^{\tau\pm}$  are given by

$$q_{n, \mathcal{S}}^{\tau\pm} = \langle \psi^\tau | \hat{q}_{n, \mathcal{S}}^\pm | \psi \rangle \quad (\mathcal{S} = \mathcal{P}, \mathcal{K}) \quad (30)$$

which resembles an expectation value as in Eq. (22), though with projection onto  $|\psi^\tau\rangle$ . The potential asymmetries  $\xi_n$  again act like sources for the alternative NLC, with  $\xi_n = \beta_n$  for real  $v_n$ . In contrast to Eq. (20), however, an  $\mathcal{ST}$ -symmetric potential now yields  $\xi_n = -\gamma_n$ , with the sources (sinks) for  $\rho_n$  representing sinks (sources) for  $\sigma_n^\tau$ . An  $\mathcal{S}$ -symmetric potential ( $\xi_n = 0$ ), on the other hand, leads to vanishing  $q_{n, \mathcal{S}}^\tau$  for energy eigenstates within a symmetry domain  $\mathbb{D}$ , even in the presence of unbalanced loss and/or gain where  $q_{n, \mathcal{S}}$  may vary spatially.

### C. Nonlocal charge evolution

The relation of *stationary* NLCs to LSS will be elaborated on in the next section. To see first the impact of the system symmetry on a general (nonstationary) state  $|\psi\rangle$  via the NLCs, let us consider the evolution of the nonlocal charge (see Eq. (19)) within a subdomain  $\mathbb{D} \subseteq \mathbb{N}$ , denoted  $\Sigma_{\psi}^{\mathbb{D}}$ , which obeys (cf. Eq. (20))

$$\partial_t \Sigma_{\psi}^{\mathbb{D}} = Q_{\mathbb{D}} + \sum_{n \in \mathbb{D}} \beta_n \sigma_n, \quad (31)$$

where  $Q_{\mathbb{D}} = \sum_{n \in \mathbb{D}} q_n$  is the total net NLC within  $\mathbb{D}$ . Now, if the *hoppings* of the system are  $\mathcal{S}_{\mathbb{D}}\mathcal{T}$ -symmetric,  $h_{\mathcal{S}(n), \mathcal{S}(n\pm 1)} = h_{n, n\pm 1}^*$ , then from the NLC expression (21) we get, in general,

$$q_{n\mp 1, \mathcal{S}}^\pm = -\eta_{n\mp 1, n}^* q_{n, \mathcal{S}}^\mp \quad (\mathcal{S} = \mathcal{P}, \mathcal{K}) \quad (32)$$

where we define the *hopping ratio*

$$\eta_{m, n} = \frac{h_{m, n}}{h_{n, m}} \quad (33)$$

between the hopping elements in opposite directions on the link  $(m, n)$ , here with  $m = n \pm 1$ . For equidirectional hoppings within  $\mathbb{D}$  we have  $\eta_{n\pm 1, n} = 1$  (as is the case for real Hermitian hoppings), so that  $Q_{\mathbb{D}}$  equals the sum  $q_{\partial\mathbb{D}}$  of currents  $q_m^{\pm}$  on links above/below sites  $m$  of the upper/lower boundaries  $\partial\mathbb{D}^{\pm}$  of  $\mathbb{D}$ ,

$$Q_{\mathbb{D}} = q_{\partial\mathbb{D}} \equiv \sum_{m \in \partial\mathbb{D}^{\pm}} q_m^{\pm}, \quad (34)$$

in the form of a nonlocal discrete Gauss law. Hence, if also the potential is  $\mathcal{S}\mathcal{T}$ -symmetric ( $\beta_{n \in \mathbb{D}} = 0$ ), the temporal change  $\partial_t \Sigma_{\psi}^{\mathbb{D}}$  in Eq.(31) is then affected only by those boundary currents  $q_{\partial\mathbb{D}}$ .

Recall that  $\mathbb{D}$  may be disconnected, being a union of distinct subdomains  $\mathbb{D}_d$  as mentioned above (after Eq.(8)), meaning that it can entail equally many  $q_m^{\pm}$  pairs at its boundary points. In the special case of *global*  $\mathcal{PT}$ -symmetry in  $\mathbb{D} = \mathbb{N}$ , we have  $\beta_n = 0$  but also  $q_{\partial\mathbb{D}} = 0$  since the boundary currents  $q_1^-, q_N^+$  vanish for the isolated array (where  $h_{1,0} = h_{N+1,N} = 0$  by definition). Thus  $Q_{\mathbb{D}=\mathbb{N}} = 0$  in Eq.(34) and thereby  $\partial_t \Sigma_{\psi}^{\mathbb{N}} = 0$ , reproducing the well-known constancy of the non-local charge (quasipower) in systems with  $\mathcal{PT}$ -symmetric potential [31, 52].

With the substitution  $\{\sigma_n, q_n, \eta_{m,n}^*\} \rightarrow \{\sigma_n^{\tau}, q_n^{\tau}, \eta_{m,n}\}$ , the above considerations can be equally applied to the evolution of a bitemporal nonlocal charge  $\Sigma_{\psi}^{\mathbb{D},\tau} = \sum_{n \in \mathbb{D}} \sigma_n^{\tau}$ . This is then constant in time for a globally  $\mathcal{P}$ -symmetric (non-Hermitian) array  $\mathbb{D} = \mathbb{N}$  with unit hopping ratios where, e. g., only lossy elements  $\gamma_n < 0$  are present.

#### IV. STATIONARY STATE INVARIANTS AND AMPLITUDE SYMMETRY MAPPING

Having established the concept of nonlocal discrete continuity in the above operator form and adapted it to symmetry mappings, we will now use the NLCs to show how LSs of the lattice system are encoded into its stationary states. The site amplitudes  $a_n$  of an eigenstate

$$|\phi\rangle = \sum_n a_n e^{-iEt} |n\rangle = e^{-iEt} |a\rangle \quad (35)$$

of the Hamiltonian with eigenvalue  $E$ ,

$$\hat{H} |\phi\rangle = E |\phi\rangle, \quad (36)$$

are given by the system of close-coupling equations

$$\begin{aligned} 0 &= h_{n,n-1} a_{n-1} + (v_n - E) a_n + h_{n,n+1} a_{n+1} \\ &\equiv g_n, \quad n \in \mathbb{N}. \end{aligned} \quad (37)$$

where the set of sites  $\mathbb{N}$  covers the system of interest: for an isolated system closed boundary conditions  $a_0 = a_{N+1} = 0$  are imposed by setting  $h_{0,1} = h_{N,N+1} = 0$ , while a scattering setup is realized by appending homogeneous semiinfinite chains with  $v_n = v$  and  $h_{n,n+1} = h$  on the left ( $n < 1$ ) and right ( $n > N$ ) of the given array (see Sec. VI). If the eigenenergy  $E$  is real, then the state  $|\phi\rangle$  is *stationary* in the sense that its local density  $\rho_n = |a_n|^2$  does not change in time. For a complex eigenenergy  $E = E^{\circ} + i\Gamma/2$  ( $E^{\circ}, \Gamma \in \mathbb{R}$ ) of a non-Hermitian  $\hat{H}$ , however, the density increases (decreases) exponentially in time as  $\rho_n = |a_n|^2 e^{\Gamma t}$  for positive (negative)  $\Gamma$  and so the state can be considered as *nonstationary*—though not containing components of distinct frequencies.

In this general case of complex  $E$ , the nonlocal continuity equation (20) for  $|\phi\rangle$  yields

$$q_n + (\beta_n - \Gamma) \sigma_n = 0. \quad (38)$$

Thus, at sites with  $\mathcal{ST}$ -symmetric onsite elements ( $\beta_n = 0$ ), a stationary state  $|\phi\rangle$  with  $\Gamma = 0$  has vanishing sum of NLC amplitudes,

$$q_{n,S} = q_{n,S}^+ + q_{n,S}^- = 0 \quad (S = \mathcal{P}, \mathcal{K}) \quad (39)$$

following a nonlocal form of a quantum Kirchoff law. For  $\mathcal{ST}$ -symmetric hoppings  $h_{n,n\pm 1}$ , the above equation can be combined with Eq.(32) to obtain

$$q_{n,S}^{\pm} = \eta_{n,n\mp 1}^* q_{n\mp 1,S}^{\pm} \quad (S = \mathcal{P}, \mathcal{K}) \quad (40)$$

for consecutive nonlocal link currents. Thus, in a *connected* domain  $\mathbb{D}$  where the system has  $\mathcal{ST}$ -symmetric Hamiltonian elements, obeying Eq.(13), the NLC  $q_{n,S}^{\pm}$  ( $q_{n,S}^{\pm}$ ) accumulates the hopping ratios as a prefactor when traversing the domain forwards (backwards). If the hoppings are complex and *Hermitian*, then  $\eta_{n,n\mp 1} = e^{2i\varphi_{n,n\mp 1}}$  and the currents accumulate a Peierls-like hopping phase factor along the path on the array. If, additionally, the hoppings are real as is the usual case in 1D setups (or generally for complex  $h_{m,n} = h_{n,m}$ , which is unusual for quantum models but relevant for, e. g., photonic arrays [51], depending on the host medium), the  $q_{n,S}^{\pm}$  are translationally *invariant*—that is, spatially constant—in  $\mathbb{D}$  for the stationary state.

For the case of  $\mathcal{S}$ -symmetry, an analogous local invariance can be derived for the two bitemporal NLCs  $q_{n,S}^{\tau\pm}$ . The associated continuity equation (28) reduces to

$$q_n^{\tau} + \xi_n \sigma_n^{\tau} = 0 \quad (41)$$

for an energy eigenstate  $|\phi\rangle$ , so that the Kirchoff law  $q_{n,S}^{\tau+} + q_{n,S}^{\tau-} = 0$  holds in a domain  $\mathbb{D}$  with  $\mathcal{S}$ -symmetric potential, that is, with  $\xi_{n \in \mathbb{D}} = 0$ . If also the hoppings are  $\mathcal{S}$ -symmetric in  $\mathbb{D}$ , then  $q_{n\mp 1,S}^{\tau\pm} = -\eta_{n\mp 1,n} q_{n,S}^{\tau\mp}$  from Eq.(29), yielding

$$q_{n,S}^{\tau\pm} = \eta_{n,n\mp 1} q_{n\mp 1,S}^{\tau\pm} \quad (S = \mathcal{P}, \mathcal{K}) \quad (42)$$

for  $n, n \pm 1 \in \mathbb{D}$ , in analogy to Eq.(32). Thus, for equidirectional hoppings ( $\eta_{n,n\mp 1} = 1$ ) the  $q_{n,S}^{\tau\pm}$  are translation invariant within the  $\mathcal{S}$ -symmetric domain  $\mathbb{D}$ , while accumulating a Peierls-like phase along it for complex Hermitian hoppings. Note that the above applies also to complex eigenenergies  $E$ , since the ‘width’  $\Gamma$  is absent in Eq.(41), and thereby to general *non-Hermitian* arrays with locally  $\mathcal{S}$ -symmetric onsite loss/gain elements.

To establish a connection between the spatial transformations and the structure of the wave amplitudes via NLCs (see Sec. IV B below), it is finally convenient to introduce an equal-time alternative to the bitemporal NLC  $q_{n,S}^{\tau\pm}$ , defined in similarity to Eq.(21) by

$$\begin{aligned} i\hat{q}_n^{\pm} &\equiv i\hat{q}_{n,S}^{\pm} \equiv i\hat{q}_{n,n\pm 1,S}^{\pm} = \\ &\psi_n h_{\mathcal{S}(n),\mathcal{S}(n\pm 1)} \psi_{\mathcal{S}(n\pm 1)} - \psi_{n\pm 1} h_{n,n\pm 1} \psi_{\mathcal{S}(n)}, \end{aligned} \quad (43)$$

simply with  $\psi_n, \psi_{n\pm 1} h_{n,n\pm 1}$  replacing their complex conjugates in  $q_{n,S}^{\pm}$ , where  $\psi_m \equiv \psi_m(t)$ . For equidirectional hoppings, they can be expressed via the NLC operators as

$$\hat{q}_{n,S}^{\pm} = \langle \psi^* | \hat{q}_{n,S} | \psi \rangle \quad (S = \mathcal{P}, \mathcal{K}) \quad (44)$$

by projecting onto the complex conjugated state  $|\psi^*\rangle \equiv \sum_n \psi_n^* |n\rangle$  (that is, without the time reversal  $t \rightarrow -t$  applied

for  $|\psi^\tau\rangle$ ). In contrast to the  $q_{n,S}^\pm$  and  $q_{n,S}^{\tau\pm}$ , the  $\hat{q}_{n,S}^\pm$  are time-dependent even for a stationary state (with  $\Gamma = 0$ ) through the harmonic factor  $e^{-2iEt}$ , and do not obey a nonlocal continuity equation like Eqs.(20) and (28). Their conditional *spatial* constancy for an energy eigenstate  $|\phi\rangle$  in an  $\mathcal{S}$ -symmetric domain  $\mathbb{D}$  can, nevertheless, be derived directly noticing that

$$i(\hat{q}_{n,S}^+ + \hat{q}_{n,S}^-) - (v_n - v_{\bar{n}})\phi_n\phi_{\bar{n}} = (a_n g_{\bar{n}} - g_n a_{\bar{n}}) e^{-2iEt} = 0 \quad (45)$$

by using the time-independent Schrödinger eigenvalue equation (37) expressed at transform-related points  $n$  and  $\bar{n} = \mathcal{S}(n)$ . The LS condition (4) together with Eq.(45) and Eq.(43) then lead to  $\hat{q}_n^\pm = \eta_{m,n\mp 1} \hat{q}_{n\mp 1}^\pm$ , just like in Eq.(42). Indeed, since  $\hat{q}_n^\pm = q_n^{\tau\pm} e^{-2iEt}$  for an energy eigenstate, it will have the same spatial characteristics as the stationary  $q_n^{\tau\pm}$ . We therefore focus on the equal-time NLCs  $q_n^\pm$  and  $\hat{q}_n^\pm$  in the remainder of the work. In the following, we list some properties of (stationary) NLCs and demonstrate their connection to the local current  $j_n^\pm$  and their use in amplitude mappings between symmetry-related sites in finite domains.

### A. Nonlocal invariants in $\mathcal{S}(\mathcal{T})$ -symmetric domains and corresponding stationary states

The ‘transfer’ relations in Eqs.(40) and (42) for the NLCs of stationary states apply quite generally for  $\mathcal{S}_{\mathbb{D}}\mathcal{T}$  and  $\mathcal{S}_{\mathbb{D}}$  symmetry, respectively, for a connected domain  $\mathbb{D} \subseteq \mathbb{N}$ . We now consider their translation invariance in the concrete case of equidirectional hoppings  $h_{n,n\pm 1} = h_{n\pm 1,n}$ , with *real* Hermitian hoppings being naturally relevant for most 1D arrays, and distinguish some basic properties as follows:

(i) In a stationary state  $|\phi\rangle$  with real energy  $E$ , local  $\mathcal{P}_{\mathbb{D}}\mathcal{T}$ -symmetry ( $v_{\bar{n}=2\alpha-n} = v_n^*$ ,  $h_{\bar{n},\bar{n}\pm 1} = h_{n,n\mp 1}^*$ ) or local  $\mathcal{K}_{\mathbb{D}}\mathcal{T}$ -symmetry ( $v_{\bar{n}=n+L} = v_n^*$ ,  $h_{\bar{n},\bar{n}\pm 1} = h_{n,n\pm 1}^*$ ) yields spatially constant corresponding currents

$$q_{n,S}^\pm = q_{\mathbb{D},S}^\pm \quad (\mathcal{S} = \mathcal{P}, \mathcal{K}) \quad (46)$$

for all  $n \in \mathbb{D}$  with  $h_{n,n\pm 1} = h_{n\pm 1,n}$ , the explicit form of the  $q_{n,S=\mathcal{P},\mathcal{K}}^\pm$  here being given by

$$i q_{n,\mathcal{P}}^\pm = h_{n,n\pm 1} (a_n^* a_{n\mp 1} - a_{n\pm 1}^* a_n), \quad (47)$$

$$i q_{n,\mathcal{K}}^\pm = h_{n,n\pm 1} (a_n^* a_{n\pm 1} - a_{n\pm 1}^* a_n), \quad (48)$$

respectively. In particular for  $\mathcal{P}_{\mathbb{D}}\mathcal{T}$  symmetry it can be shown that  $q_{\mathbb{D},\mathcal{P}}^\pm$  vanishes for a state vector  $\phi$  whose part  $\phi_{\mathbb{D}} = \{\phi_n \in \mathbb{D}\}$  is a local  $\mathcal{PT}$  ‘eigenstate’, and *vice versa*, that is,

$$\phi_n^* = \lambda_{\mathbb{D},\mathcal{PT}} \phi_n, \quad n \in \mathbb{D} \iff q_{\mathbb{D},\mathcal{P}}^\pm = 0, \quad (49)$$

with unimodular ‘eigenvalue’,  $|\lambda_{\mathbb{D},\mathcal{PT}}| = 1$ , which in turn corresponds to locally symmetric density  $\rho_n$  within  $\mathbb{D}$ . In fact, this applies for arbitrary  $\mathcal{P}_{\mathbb{D}}\mathcal{T}$ -symmetric hoppings, since no hopping ratio is accumulated in Eq.(40) for zero current. For the (local)  $\mathcal{PT}$  eigenstate above it further holds that

$$\lambda_{\mathbb{D},\mathcal{PT}} \hat{q}_{n,\mathcal{P}}^\pm = -j_n^\pm = j_{\bar{n}}^\mp, \quad (50)$$

connecting the alternative nonlocal current with the local one.

(ii) For local  $\mathcal{P}_{\mathbb{D}}$ -symmetry ( $v_{\bar{n}=2\alpha-n} = v_n$ ,  $h_{\bar{n},\bar{n}\pm 1} = h_{n,n\mp 1}$ ) or local  $\mathcal{K}_{\mathbb{D}}$ -symmetry ( $v_{\bar{n}=L+n} = v_n$ ,  $h_{\bar{n},\bar{n}\pm 1} =$

$h_{n,n\pm 1}$ ), the alternative (time-dependent) quantities  $\hat{q}_{n,S}^\pm$  are spatially constant in  $\mathbb{D}$ ,

$$\hat{q}_{n,S}^\pm = \hat{q}_{\mathbb{D},S}^\pm \quad (\mathcal{S} = \mathcal{P}, \mathcal{K}) \quad (51)$$

with their explicit form for  $|\phi\rangle$  given by

$$i \hat{q}_{n,\mathcal{P}}^\pm = h_{n,n\pm 1} (a_n a_{n\mp 1} - a_{n\pm 1} a_n) e^{2iEt}, \quad (52)$$

$$i \hat{q}_{n,\mathcal{K}}^\pm = h_{n,n\pm 1} (a_n a_{n\pm 1} - a_{n\pm 1} a_n) e^{2iEt}, \quad (53)$$

respectively. We underline that those invariants exist also for non-Hermitian  $\mathcal{S}_{\mathbb{D}}$ -symmetric potentials, e. g. with (locally) symmetric loss profile or ‘unbalanced’ loss/gain elements. In analogy to Eq.(49),  $\hat{q}_{\mathbb{D},\mathcal{P}}^\pm$  vanishes iff the part  $\phi_{\mathbb{D}}$  is a local  $\mathcal{P}$  ‘eigenstate’,

$$\phi_{\bar{n}} = \lambda_{\mathbb{D},\mathcal{P}} \phi_n, \quad n \in \mathbb{D} \iff \hat{q}_{\mathbb{D},\mathcal{P}}^\pm = 0, \quad (54)$$

now with eigenvalue  $\lambda_{\mathbb{D},\mathcal{P}} = \pm 1$ , and then also

$$\lambda_{\mathbb{D},\mathcal{P}} q_{n,\mathcal{P}}^\pm = j_n^\pm = j_{\bar{n}}^\mp \quad (55)$$

holds for the NLC (recall that generally  $j_n^\pm \neq 0$  even for a finite array in the presence of sources and/or sinks). Again  $\rho_n$  is locally symmetric in  $\mathbb{D}$  for arbitrary  $\mathcal{P}_{\mathbb{D}}$ -symmetric hoppings. Note that, for real Hermitian  $\hat{H}$ , Eqs.(49) and (54) are equally applicable for bound arrays and for scattering. An application of the latter in relation to perfect transmission is addressed in Sec.VI.

(iii) For a general state  $|\psi\rangle$ , the NLC and its alternative are by construction  $\mathcal{P}_{\mathbb{D}}\mathcal{T}$ -symmetric and  $\mathcal{P}_{\mathbb{D}}$ -antisymmetric, respectively,

$$q_{n,\mathcal{P}}^\pm = q_{\bar{n},\mathcal{P}}^{\mp*} \quad \text{and} \quad \hat{q}_{n,\mathcal{P}}^\pm = -\hat{q}_{\bar{n},\mathcal{P}}^{\mp*}, \quad (56)$$

noting that the link  $(n, n \pm 1)$  is  $\mathcal{P}$ -mapped to  $(\bar{n}, \bar{n} \mp 1)$ . If the hoppings  $h_{n,n\pm 1}$  are equidirectional (real Hermitian in practice) and  $\mathcal{P}_{\mathbb{D}}\mathcal{T}$ - or  $\mathcal{P}_{\mathbb{D}}$ -symmetric, then we further have that

$$q_{\bar{n}\mp 1,\mathcal{P}}^\pm = -q_{n,\mathcal{P}}^{\pm*} \quad \text{or} \quad \hat{q}_{\bar{n}\mp 1,\mathcal{P}}^\pm = \hat{q}_{n,\mathcal{P}}^\pm \quad (57)$$

within  $\mathbb{D}$ , respectively, for *arbitrary* onsite elements  $v_n$ . Thus, the  $|q_{n,\mathcal{P}}^\pm|$  or  $|\hat{q}_{n,\mathcal{P}}^\pm|$  are then locally symmetric about the center  $\alpha$  (that is, about the shifted center  $\alpha \mp \frac{1}{2}$  if assigned to sites) for any complex potential profile, regardless of its symmetry. If the potential is  $\mathcal{P}_{\mathbb{D}}\mathcal{T}$ -symmetric ( $\mathcal{P}_{\mathbb{D}}$ -symmetric), then the first equation above together with the spatial constancy, Eq.(46), of the  $q_{n,\mathcal{P}}^\pm$  for an energy eigenstate  $|\phi\rangle$  with real (complex)  $E$  implies that they are imaginary,  $q_{n,\mathcal{P}}^\pm \in i\mathbb{R}$ .

(iv) For an eigenstate (Bloch state)  $|\phi^k\rangle$  of the finite translation operator  $\hat{K}$  with wavefunction  $\phi_n^k = e^{ikn} \chi_n^k$ , where  $\chi_n^k = \chi_{n+L}^k$ , the associated NLC equals the local current times the Bloch factor while its alternative vanishes,

$$q_{n,\mathcal{K}}^\pm = j_n^\pm e^{ikL}, \quad \hat{q}_{n,\mathcal{K}}^\pm = 0. \quad (58)$$

This applies for energy eigenstates of globally  $\mathcal{K}$ -symmetric systems of period  $L$  with symmetry domain  $\mathbb{D} = \mathbb{N}$ , including finite ring structures (where site  $n = N$  is coupled to site  $n = 1$ ). Recall here that a  $\mathcal{KT}$ -symmetric potential, where the  $q_{n,\mathcal{K}}^\pm$  above may be spatially constant, has period  $L$  only if it is real (whereby it is  $\mathcal{K}$ -symmetric), in which case also the  $j_n^\pm$  are conserved.

(v) The NLCs for a forward translation  $\mathcal{K}^+(n) = \bar{n} = n + L$  in a general state  $|\psi\rangle$  are related to those for a backward translation  $\mathcal{K}^-(n) = n - L$  from the mapped site  $\bar{n}$  by

$$q_{n,\mathcal{K}^+}^\pm = -q_{\bar{n},\mathcal{K}^-}^{\mp*}, \quad \hat{q}_{n,\mathcal{K}^+}^\pm = -\hat{q}_{\bar{n},\mathcal{K}^-}^{\mp*} \quad (59)$$

for  $\mathcal{KT}$ - and  $\mathcal{K}$ -symmetric equidirectional hoppings, respectively. Thus, for a stationary state (with real  $E$ ), although the  $q_{n,\mathcal{K}^+}^\pm$  are constant only in the subdomain  $\mathbb{D}$  of a locally  $\mathcal{KT}$ -symmetric domain  $\mathbb{U} = \mathbb{D} \cup \mathbb{L}$  (see Fig. 1), we can assign  $-q_{n,\mathcal{K}^-}^{\mp*} = q_{n-L,\mathcal{K}^+}^\pm = q_{\mathbb{D},\mathcal{K}^+}^\pm$  to (links from) sites  $n$  in the last period  $\mathbb{L}$ , and similarly for  $\mathcal{K}$  symmetry and the  $\hat{q}_{n,\mathcal{K}^+}^\pm$ . This way the symmetry is expressed by nonlocal invariants throughout the whole domain  $\mathbb{U}$ .

## B. Amplitude mapping and current connection

The wave amplitude  $\psi_{\mathcal{S}(n)}$  at the transformed site is related to that of the original one  $\psi_n$  and its conjugate via the  $q_{n,\mathcal{S}}^\pm, \hat{q}_{n,\mathcal{S}}^\pm, j_n^\pm$  through the general identity

$$\psi_{\mathcal{S}(n)} = \frac{1}{j_n^\pm} \left( q_{n,\mathcal{S}}^\pm \psi_n - \hat{q}_{n,\mathcal{S}}^\pm \psi_n^* \right), \quad (60)$$

holding for arbitrary  $\hat{H}$ , where both the upper and lower sign in  $\pm$  can be chosen; see derivation in Appendix B. For locally  $\mathcal{S}$ -symmetric and real equidirectional hoppings  $h_{n,n\pm 1} = h_{n,\mathcal{S}(n),\mathcal{S}(n\pm 1)}^*$  ( $n \in \mathbb{D}$ ), also the *neighboring* amplitudes at  $n \pm 1$  and  $\mathcal{S}(n \pm 1)$  are related via the *same* currents (now with corresponding sign in  $\pm$ ); see Eq. (B2). In other words we have  $j_n^\pm \psi_{\mathcal{S}(n)} = [q_{n,\mathcal{S}}^\pm, -\hat{q}_{n,\mathcal{S}}^\pm][\psi_n, \psi_n^*]^\top = [q_{n\mp 1,\mathcal{S}}^\pm, -\hat{q}_{n\mp 1,\mathcal{S}}^\pm][\psi_n, \psi_n^*]^\top$ , so that the  $\mathcal{S}$ -transformed amplitudes at  $n, \mathcal{S}(n)$  are related by *both*  $\pm$  NLCs ‘flowing’ on *either* of the attached link pairs  $(n, n \pm 1), (\mathcal{S}(n), \mathcal{S}(n \pm 1))$ ; see nonlocal ‘flow’ in Fig. 2.

If, further, the potential  $v_n$  is both  $\mathcal{S}_{\mathbb{D}}\mathcal{T}$ - and  $\mathcal{S}_{\mathbb{D}}$ -symmetric (that is, real and  $\mathcal{S}_{\mathbb{D}}$ -symmetric), then both  $q_{n,\mathcal{S}}^\pm = q_{\mathbb{D},\mathcal{S}}^\pm$  and  $\hat{q}_{n,\mathcal{S}}^\pm = \hat{q}_{\mathbb{D},\mathcal{S}}^\pm$ , as well as  $j_n^\pm = j_{\mathbb{D}}^\pm$ , are spatially constant within  $\mathbb{D}$  for a stationary state  $|\phi\rangle$ . Hence, Eq. (60) becomes

$$\phi_{\mathcal{S}(n)} = \frac{q_{\mathbb{D},\mathcal{S}}^\pm}{j_{\mathbb{D}}^\pm} \phi_n - \frac{\hat{q}_{\mathbb{D},\mathcal{S}}^\pm}{j_{\mathbb{D}}^\pm} \phi_n^* \quad (61)$$

for all  $n$  in  $\mathbb{D}$ , providing a linear *mapping relation* from  $\phi_n, \phi_n^*$  to  $\phi_{\mathcal{S}(n)}$  with constant coefficients  $q_{\mathbb{D},\mathcal{S}}^\pm/j_{\mathbb{D}}^\pm$  and  $\hat{q}_{\mathbb{D},\mathcal{S}}^\pm/j_{\mathbb{D}}^\pm$  which can be evaluated for any link  $(n, n \pm 1)$  in  $\mathbb{D}$ . Note that the same stationary mapping of Eq. (61) would be arrived at by formulating the identity in Eq. (60) using the bitemporal NLC  $q_{n,\mathcal{S}}^{\mp*}$  instead of  $\hat{q}_{n,\mathcal{S}}^\pm$ ; see Appendix B.

This mapping is clearly not applicable for real spatial components  $a_n$  of  $|\phi\rangle$  in  $\mathbb{D}$  (or trivially complex through a common prefactor), since the  $j_{\mathbb{D}}^\pm$  then vanish. At the same time, real  $a_n$  yield equimodular  $q_{n,\mathcal{S}}^\pm$  and  $\hat{q}_{n,\mathcal{S}}^\pm$ , which in turn coincides quite generally with vanishing local current. Indeed, a general identity connecting the nonlocal and local currents on links to sites  $n$  and  $\bar{n} = \mathcal{S}(n)$  is (see Appendix B)

$$|q_{n,\mathcal{S}}^\pm|^2 - |\hat{q}_{n,\mathcal{S}}^\pm|^2 = j_n^\pm j_{\mathcal{S}(n)}^{\pm s} \quad (62)$$

with the sign  $s = -, +$  for  $\mathcal{S} = \mathcal{P}, \mathcal{K}$ , respectively, implying  $j_{\mathcal{P}(n)}^\mp = j_{\mathcal{P}(n),\mathcal{P}(n\pm 1)}$  and  $j_{\mathcal{K}(n)}^\mp = j_{\mathcal{K}(n),\mathcal{K}(n\pm 1)}$ . This *current connection* holds also for  $j_n^\pm = 0$ , in which case  $\hat{q}_{n,\mathcal{S}}^\pm = e^{2i\theta_n} q_{n,\mathcal{S}}^\pm$ , where  $\theta_n$  is the phase of the general wavefunction

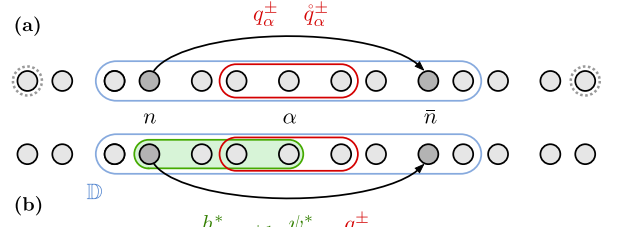


FIG. 3. Symmetry-induced domain amplitude mapping: Within a locally  $\mathcal{P}$ -symmetric subdomain (blue line) of a 1D array, the amplitude at site  $n$  is mapped to its image at  $\bar{n}$ , as indicated by arrows together with the quantities required for the mapping. (a) Current mapping via Eq. (61) in terms of translation invariant local currents  $j_n^\pm$  and NLCs  $q_n^\pm, \hat{q}_n^\pm$  evaluated at  $n = \alpha$  using  $a_\alpha$  and  $a_{\alpha\pm 1}$  (red line). Dotted contour on end sites indicate current flow to ensure  $j_n^\pm \neq 0$ . (b) Summation mapping via Eq. (67) in terms of amplitudes and couplings up to the domain center  $\alpha$  (green line) and the domain invariant  $q_\alpha^\pm$ .

$\psi_n = |\psi_n|e^{i\theta_n}$ , as can easily be checked. For a stationary state we further have that  $j_n^\pm j_{\mathcal{S}(n)}^\pm = (j_n^\pm)^2 \equiv (j_{\mathbb{U}}^\pm)^2$  within a Hermitian domain  $\mathbb{U} \ni n, \mathcal{S}(n)$ . Thus, the wave amplitudes in *different* local  $\mathcal{ST}$  or  $\mathcal{S}$  symmetry domains  $\mathbb{D}_d$  ( $d = 1, 2, \dots$ ) in a globally Hermitian system are interrelated by common differences  $|q_{\mathbb{D}_1,\mathcal{S}}^\pm|^2 - |\hat{q}_{\mathbb{D}_1,\mathcal{S}}^\pm|^2 = |q_{\mathbb{D}_2,\mathcal{S}}^\pm|^2 - |\hat{q}_{\mathbb{D}_2,\mathcal{S}}^\pm|^2 = \dots = |j_{\mathbb{N}}^\pm|^2$  through Eq. (62) for  $\mathcal{S} = \mathcal{P}, \mathcal{K}$ .

Considering  $\mathcal{S}$ -symmetry, the mapping relation (61) can be seen as a generalization of the parity and Bloch theorems (which map amplitudes to a symmetry-related site via the associated eigenvalue) from global to local  $\mathcal{P}$ - and  $\mathcal{K}$ -symmetry, respectively, where breaking of the global symmetry adds an admixture of the complex conjugate  $\phi_n^*$  to the mapping. Taking the continuum limit  $\ell \rightarrow 0$  (setting all hoppings equal), Eq. (61) reproduces the generalized Bloch and parity theorems of Ref. [25] for stationary states. Those are here extended to non-Hermitian Hamiltonians with variable hoppings and are shown to follow from the general identity (60) for arbitrary states. The usual (global) versions  $\phi_{\mathcal{P}(n)} = \pm \phi_n$  or  $\phi_{\mathcal{K}(n)} = e^{ikL} \phi_n$  are recovered directly by inserting Eqs. (54),(55) or Eq. (58) with  $\mathbb{D} = \mathbb{N}$  for a parity or Bloch eigenstate, respectively, into Eq. (61) (or Eqs. (49),(50) for a  $\mathcal{PT}$  eigenstate). Note that, to avoid  $j_n^\pm = 0$  for  $\mathcal{P}$  eigenstates, a non-Hermitian  $\mathcal{P}$ -symmetric system can be considered, subsequently taking the limit of vanishing loss/gain to reproduce the Hermitian case.

## C. Summation amplitude mapping

Although the identity of the current connection in Eq. (62) holds for any Hamiltonian  $\hat{H}$  and any state  $|\psi\rangle$ , the mapping relation of Eq. (60)—and its form for a stationary state within a locally symmetric domain, Eq. (61)—are applicable only for nonzero local current. This is realized in 1D systems for a scattering setting with open boundaries (connected to asymptotic leads, see Sec. VI) through which current flows, or for a finite setup with current sources and/or sinks (see VB), where the field amplitudes  $a_m$  in stationary states are (nontrivially) complex.

We now show that the NLCs (which generally do not vanish even if the local current does) can be used to map also *real* amplitudes of bound Hermitian systems between remote sites, thereby exploiting the information of LS. Indeed, assuming  $\mathcal{PT}$ -symmetric hoppings  $h_{\mathcal{S}(n),\mathcal{S}(n\pm 1)} = h_{n,n\pm 1}^*$  for  $n \in \mathbb{D}$ ,

we notice that the NLCs  $q_n^\pm$  for a state  $|\psi\rangle$  can be written (times  $i$ ) as

$$iq_n^\pm = h_{n,n\pm 1}^* (\psi_n^* \Delta^\pm \psi_{\bar{n}} - \psi_{\bar{n}} \Delta^\pm \psi_n^*) \quad (63)$$

$$= h_{n,n\pm 1}^* \psi_n^* \psi_{n+1}^* \Delta^\pm \left( \frac{\psi_{\bar{n}}}{\psi_n^*} \right), \quad (64)$$

with the forward/backward discrete difference operator  $\Delta^\pm$  defined here by

$$\Delta^\pm \psi_{f(n)} = \psi_{f(n\pm 1)} - \psi_n \quad (65)$$

for any mapping  $f(n)$  (set to  $f(n) = n$  or  $f(n) = \bar{n} = \mathcal{S}(n)$  above). Summing the discrete quotient difference [53] in Eq. (64) from site  $n$  to  $n_0 \mp 1$  for a given site  $n_0$  and solving for the mapped amplitude  $\psi_{\bar{n}}$  we obtain

$$\psi_{\bar{n}} = \psi_n^* \left( \frac{\psi_{\bar{n}_0}}{\psi_{n_0}^*} - i \sum_{m=n}^{n_0 \mp 1} \frac{q_m^\pm}{\psi_m^* h_{m,m\pm 1}^* \psi_{m\pm 1}^*} \right), \quad (66)$$

applicable for nonzero  $\psi_{n_0}, \psi_m, \psi_{m\pm 1}$ . Hence, in the case of real amplitudes  $a_n$  of a stationary state  $|\phi\rangle$  within a locally  $\mathcal{PT}$ -symmetric domain  $\mathbb{D}$  with odd number of sites  $D$ , choosing the fixed point to be the symmetry center  $n_0 = \alpha$  (so that  $a_{\bar{n}_0} = a_{n_0}$ ) simplifies the above expression to

$$a_{\bar{n}} = a_n \left( 1 - iq_{\mathbb{D}}^+ \sum_{m=n}^{\alpha-1} \frac{1}{a_m h_{m,m+1}^* a_{m+1}} \right), \quad (67)$$

where  $q_{\mathbb{D}}^+$  is the symmetry-induced invariant in  $\mathbb{D}$  (with the upper sign selected here). In this manner the image amplitudes  $a_{\bar{n}}$  can be determined from multiple  $a_n$ 's (including the  $a_{\alpha\pm 1}$  needed to evaluate  $q_{\mathbb{D}}^+ = q_\alpha^+$ ); see Fig. 3. The same can be done for an odd-sized  $\mathcal{P}$ -symmetric domain, correspondingly using  $q_{\mathbb{D}}^+$  and  $a_m, h_{m,m+1}$  in Eq. (67). In other cases (e.g.  $\mathcal{P}(\mathcal{T})$  symmetry with even  $D$ , or  $\mathcal{K}(\mathcal{T})$  symmetry), Eq. (66) yields the amplitude mapping provided that the quotient  $a_{\bar{n}_0}/a_{n_0}$  can be previously determined. The summation mapping presented here holds also for zero current (implying real  $h_{n,n+1}$  for real  $a_n$ ) and can thus be seen as a complement to the current mapping in Eq. (60).

#### D. Invariants in periodically modulated systems

For a time-dependent Hamiltonian  $\hat{H}(t)$  (equivalently, varying along the longitudinal direction  $z$  of a photonic waveguide array), there are no stationary eigenstates and so no spatially invariant NLCs in symmetry domains. In the case, however, of a *periodic* modulation with frequency  $\omega$ ,

$$\hat{H}(t) = \hat{H}(t + \tau), \quad \tau = 2\pi/\omega, \quad (68)$$

the Schrödinger equation (2) admits solutions of the form

$$|\psi^\mu(t)\rangle = e^{-i\epsilon_\mu t} |\phi^\mu(t)\rangle, \quad |\phi^\mu(t)\rangle = |\phi^\mu(t + \tau)\rangle, \quad (69)$$

where the real quasienergies  $\epsilon_\mu$  (named in analogy to the quasimomentum of Bloch states in spatially periodic systems) are defined up to multiples of  $2\pi$ . Being *quasi*-stationary eigenstates of the modified Hamiltonian operator  $\hat{H}_F = \hat{H} - i\partial_t$  with eigenvalues  $\epsilon_\mu$ , the periodic Floquet modes  $|\phi^\mu(t)\rangle$  suggest the existence of a type of nonlocal invariants within spatially symmetric domains, in analogy to those for stationary states of a static  $\hat{H}$ . Indeed, integrating the nonlocal continuity Eq. (20) in a Floquet state  $|\psi^\mu\rangle$  over one period  $\tau$  for a

potential  $v_n(t)$  (assumed real for simplicity) which is locally  $\mathcal{S}$ -symmetric at any  $t$ ,  $v_{\bar{n}}(t) = v_n(t)$ , we obtain

$$\bar{q}_{n;\mu} \equiv \bar{q}_{n;\mu}^+ + \bar{q}_{n;\mu}^- = [\sigma_{n;\mu}(t)]_0^\tau = 0 \quad (70)$$

since  $\sigma_{n;\mu}(t) = \langle \psi^\mu(t) | \hat{\sigma}_n | \psi^\mu(t) \rangle$  is periodic, where

$$\bar{q}_{n;\mu}^\pm = \frac{1}{\tau} \int_0^\tau dt q_{n;\mu}^\pm(t) \quad (71)$$

are the period-averaged NLCs in state  $|\psi^\mu\rangle$  of the  $\mathcal{S}$ -related links  $(n, n\pm 1)$ ,  $(\mathcal{S}(n), \mathcal{S}(n\pm 1))$ . Just like in the case of static  $\hat{H}$ , we have  $\bar{q}_{n\mp 1;\mu}^\pm = \bar{q}_{n;\mu}^\pm$  for equidirectional (assumed real)  $\mathcal{S}$ -symmetric hoppings  $h_{\mathcal{S}(n), \mathcal{S}(n\pm 1)} = h_{n, n\pm 1}$ , so that the  $\bar{q}_{n;\mu}^\pm$  are spatially constant in the domain of symmetry  $\mathbb{D}$ ; cf. Eq. (40). This generalizes the characterization of the LSs by associated invariants to 1D systems driven periodically with arbitrary strength. Like their static counterpart, the period invariants  $\bar{q}_{n;\mu}^\pm$  also exist independently of boundary conditions; they will be illustrated in an example with bound Floquet modes in Sec. VC.

## V. NONLOCAL CURRENTS OF BOUND EIGENMODES

Having established the framework of LS operations, nonlocal current-density continuity and symmetry-induced stationary nonlocal 1D invariants, we now address the occurrence of the latter invariants in bound systems, that is, finite arrays  $\mathbb{N}$  of  $N$  sites. We first illustrate the various types of LS in 1D, then show how the NLCs relate to symmetry breaking in globally  $\mathcal{ST}$ -symmetric non-Hermitian setups, and finally give an example of nonlocal invariants of bound quasistationary modes in a periodically modulated array. In the remainder of the paper, lengths, field amplitudes and  $\mathcal{H}$ -elements are measured in units of  $\ell$  (lattice constant),  $a^\circ$  (amplitude unit) and  $\epsilon$  ( $\mathcal{H}$ -element unit), respectively, which are in turn set to unity,  $\ell = a^\circ = \epsilon = 1$ .

### A. Types of local symmetry

We consider an array of  $N = 15$  sites, large enough to encompass different types of symmetry (global, complete, overlapping, and gapped; see below) under local reflection or translation operations. Choosing real onsite elements  $v_n = u_n$  and real equidistant closest-neighbor hoppings  $h_{n, n\pm 1}$ , the mode amplitudes  $a_n^\nu$  of an eigenstate  $|\phi^\nu\rangle = \sum_n \phi_n^\nu |n\rangle = \sum_n a_n^\nu e^{-iE_\nu t} |n\rangle$  with eigenvalue  $E_\nu$  ( $\nu = 1, 2, \dots, N$ ) can also be chosen real. The NLCs

$$q_{n;\psi}^\pm = \sum_\nu |c_\nu|^2 q_{n;\nu}^\pm + \sum_\nu \sum_{\mu \neq \nu} c_\nu^* c_\mu q_{n;\nu\mu}^\pm \quad (72)$$

in a general state (wavepacket)  $|\psi\rangle = \sum_\nu c_\nu |\phi^\nu\rangle$  are composed of a linear combination of the  $q_{n;\nu}^\pm$  of individual modes  $\nu$  as well as mixed-mode currents  $i q_{n;\nu\mu}^\pm \equiv \phi_n^{\nu*} h_{\mathcal{S}(n), \mathcal{S}(n\pm 1)} \phi_{\mathcal{S}(n\pm 1)}^\mu - \phi_{n\pm 1}^{\nu*} h_{n, n\pm 1}^* \phi_{\mathcal{S}(n)}^\mu$  ( $\mathcal{S} = \mathcal{P}, \mathcal{K}$ ) which oscillate with frequency  $E_\nu - E_\mu$ . All general statements of Secs. IIIB and IV about NLCs of general states  $|\psi\rangle$  apply to  $q_{n;\psi}^\pm$ , while, in particular, the stationary currents  $q_{n;\nu}^\pm$  are additionally translation invariant in a corresponding LS domain  $\mathbb{D}$ . In the following, we discuss the different types of local  $\mathcal{P}$ - and  $\mathcal{K}$ -symmetry in terms of the example arrays shown in Fig. 4 together with the locally

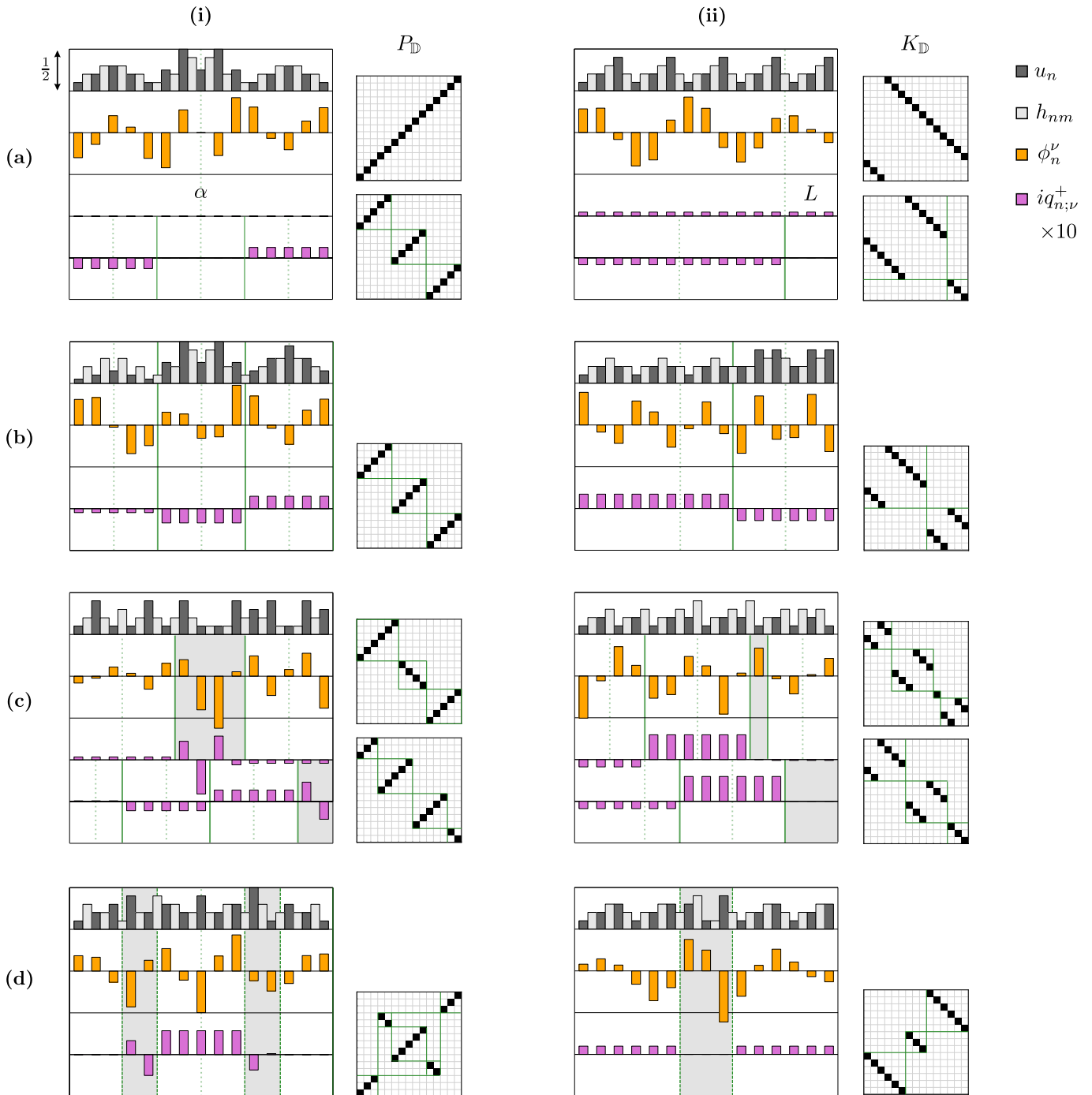


FIG. 4. Types of local symmetry (LS) and corresponding local permutation matrices for (i) inversion and (ii) translation transforms for finite 1D arrays of  $N = 15$  sites. Plotted quantities (indicated in legend) are: real onsite potential  $u_n$  (dark gray), real hoppings  $h_{nm}$  between sites (light gray), eigenmode amplitudes  $\phi_n^\nu$  (orange),  $10i$  times imaginary NLC  $q_{n,\nu}^+$  of mode  $\nu$  (purple). (a) Global symmetry within  $\mathbb{U} = \mathbb{N}$ , where  $\mathbb{N}$  covers the complete system, (b) complete LS (CLS) in nonoverlapping subdomains  $\mathbb{D}_d \subset \mathbb{N} = \bigcup_d \mathbb{D}_d$ , (c) overlapping LS for two different LS operations, and (d) gapped symmetry within  $\mathbb{U} = \mathbb{N}$ . Eigenmodes (i)  $\nu = 8, 7, 9, 7$  and (ii)  $\nu = 6, 10, 8, 6$  for (a,b,c,d), respectively, were chosen with visibly distinct  $q_{\mathbb{D}_d}^+$  as a criterion. In (a,i) and (a,ii) the  $q_{\mathbb{D}_d}^+$  for a LS transform are additionally shown. In order to illustrate their domainwise constancy, the (upper) NLCs are plotted at the sites  $n$  below the links  $(n, n+1)$  they are defined on. In (ii), backward invariants  $-q_{n,\mathcal{K}}^*$  are plotted in the last period of each LS domain; see Eq. (59). Solid vertical lines indicate LS domains, dotted lines the local (i) inversion points  $\alpha_d$  and (ii) translation lengths  $L_d$ . Shaded areas indicate lack of symmetry under the considered transform. All plotted quantities are dimensionless, with each panel row being of height  $1/2$ , as indicated on the upper left in (a,i).

invariant  $q_{n,\nu}^\pm$  for selected modes  $|\phi^\nu\rangle$  as well as the  $\mathcal{P}_\mathbb{D}$ - and  $\mathcal{K}_\mathbb{D}$ -matrices producing them via Eq. (26).

**(a) Global symmetry.** In the case of global symmetry, there is a connected maximal symmetry domain  $\mathbb{U} = \mathbb{N}$  which extends over the complete setup. We call a (local) symmetry

maximal [12] if the corresponding domain  $\mathbb{U} = \mathbb{D} \cup \bar{\mathbb{D}}$  is the largest one with the given center  $\alpha$  (for  $\mathcal{P}$  symmetry) or period  $L$  (for  $\mathcal{K}$  symmetry). In the case of global  $\mathcal{P}$  symmetry, shown in Fig. 4 (a,i), the corresponding permutation matrix  $P_\mathbb{D} = P_\mathbb{N}$  is the usual anti-diagonal unit matrix (upper inset), and the  $q_{n,\nu}^\pm$  vanish for any mode  $|\phi^\nu\rangle$  due to its definite parity

(see Eq. (49)). If  $\mathbb{N}$  contains a subdomain  $\mathbb{D}_1$  which is locally  $\mathcal{P}_{\mathbb{D}_1}$ -symmetric, then its image  $\mathcal{P}(\mathbb{D}_1)$  under the global inversion has opposite invariants  $q_{\mathcal{P}(\mathbb{D}_1); \nu}^{\pm} = -q_{\mathbb{D}_1; \nu}^{\pm}$ , as seen in the lower panel of Fig. 4 (a,i) together with the corresponding local inversion matrix (lower inset).

We call a finite system ‘globally’  $\mathcal{K}$ -symmetric here by convention if it is periodic in  $\mathbb{U} = \mathbb{D} \cup \mathbb{L} = \mathbb{N}$ , that is, if it consists of repeated copies of a given last period  $\mathbb{L}$ , as shown in Fig. 4 (a,ii); a ‘truly’ globally  $\mathcal{K}$ -symmetric array is infinite with  $\mathbb{D} = \mathbb{N}$ . Due to the finiteness of  $\mathbb{N}$ , the  $q_{n; \nu}^{\pm}$  with  $n \in \mathbb{L}$  differ from the invariants in  $\mathbb{D}$  (resulting from the inhomogeneity of the global  $K_{\mathbb{D}}$ -matrix; see upper inset), and therefore we assign the backward invariants  $-q_{n; \mathcal{K}}^{\mp*}$  (see Eq. (59)) to  $\mathbb{L}$  in order to illustrate the  $\mathcal{K}_{\mathbb{D}}$ -symmetry. A locally  $\mathcal{K}_{\mathbb{D}_1}$ -symmetric subdomain of  $\mathbb{N}$  with different period  $L_1 \neq L$  also leads to different currents, as seen in the lower panel of Fig. 4 (a,ii).

**(b) Complete local symmetry.** In the case of complete LS (CLS), the setup is exactly covered by more than one maximal non-overlapping symmetry domains  $\mathbb{U}_d$ , that is,  $\mathbb{N} = \mathbb{U} = \bigcup_d \mathbb{U}_d$  with  $\mathbb{U}_d \cap \mathbb{U}_{d'} = \emptyset$ , as exemplified in Fig. 4 (b) for local (i)  $\mathcal{P}$  and (ii)  $\mathcal{K}$  symmetry, excluding here the trivial case of single-site (size  $D_d = 1$ ) domains. The corresponding  $P_{\mathbb{D}}$ - and  $K_{\mathbb{D}}$ -matrices are block-diagonal with the blocks being local inversion (exchange) and translation (cyclic shift) permutation matrices; see insets. In this class of systems, the local order of the Hamiltonian is completely mapped via its eigenstates to the domain invariants  $q_{\mathbb{D}_d; \nu}^{\pm}$  which in this sense expose the symmetry information encoded in the states  $|\phi^{\nu}\rangle$ . Note that, for both local  $\mathcal{P}$  and  $\mathcal{K}$  symmetry, this information is otherwise not at all visible by the mode amplitude profiles alone for an arbitrary CLS setup. Considering extended lattice systems of large size  $N$ , the concept of CLS and associated LS-induced invariants may serve to characterize order between the limits of perfect periodicity and uncorrelated disorder, though different from that of quasiperiodicity (or deterministic aperiodicity) [12]. Here, the component of disorder may be present in arbitrary amount, within the LS domain themselves or at the level of their distribution in the system.

**(c) Overlapping local symmetry.** The case of overlapping LS refers to the existence of *different* symmetry domains of the same setup with common sites, that is, there are (composite) LS domains  $\mathbb{U} = \bigcup_d \mathbb{U}_d$  and  $\mathbb{U}' = \bigcup_{d'} \mathbb{U}'_{d'}$  with  $\mathbb{U}_d \neq \mathbb{U}'_{d'}$  but  $\mathbb{U}_d \cap \mathbb{U}'_{d'} \neq \emptyset$  for some  $\mathbb{U}_d, \mathbb{U}'_{d'}$ . Examples of non-CLS setups with overlapping  $\mathcal{P}$ - and  $\mathcal{K}$ -symmetric domains are shown in Fig. 4 (c,i) and (c,ii), respectively. Note that overlapping  $\mathcal{P}$ -symmetric domains with common center  $\alpha$  or  $\mathcal{K}$ -symmetric domains with common period  $\mathbb{L}$  have equal invariant currents  $q_{n; \nu}^{\pm}$ , respectively. In general, a setup may contain mixed local  $\mathcal{P}$  and  $\mathcal{K}$  symmetries in different domains which in turn may overlap (an obvious case being a  $\mathcal{K}$ -symmetric array with  $\mathcal{P}$ -symmetric period), and the concept of overlapping LS may be used to analyze order in complex systems at different scales [12]. If overlapping LS domains occur in a CLS system, then we speak of different CLS *decompositions* of the system. As has been shown for continuous models [27], scattering setups with multiple complete local  $\mathcal{P}$ -symmetry decompositions can enable the design of transparency at multiple incoming frequencies for generic globally  $\mathcal{P}$ -asymmetric scatterers.

**(d) Gapped (local) symmetry.** If the Hamiltonian elements in

one (or more than one) subdomain(s) of a LS domain  $\mathbb{D}$  is modified so that it no longer obeys the considered symmetry (with a given  $\mathcal{P}$ -center or  $\mathcal{K}$ -period), then the original symmetry domain becomes disconnected, or ‘gapped’, as illustrated in Fig. 4 (d). The  $q_{n; \nu}^{\pm}$  are then spatially constant in the symmetric subparts of  $\mathbb{D}$  outside the gap(s), but generally unequal in different subparts (recall that the translational invariance of  $q_{n; \nu}^{\pm}$ , pertaining from Eq. (40), relies on the connectedness of the LS domain). In the case of gapped  $\mathcal{P}$  symmetry, however, the identity (57) between symmetry-related currents yield equal  $q_{n; \nu}^{\pm}$  at symmetry-related subparts for real amplitudes  $a_n$ , in spite of the intervening asymmetric gaps. This is seen in Fig. 4 (d,i), where the unconnected symmetry-related left and right ends have equal (vanishing)  $q_{n; \nu}^{\pm}$ . In the case of gapped  $\mathcal{K}$  symmetry, the gap(s) induce distinct constant  $q_{n; \nu}^{\pm}$ ’s in each unperturbed part of each gapped period. The example in Fig. 4 (d,ii) shows the constancy of  $q_{n; \nu}^{\pm}$  in a gapped single-period domain (the subpart of the first 6 sites of the period  $L = 9$  is repeated after the gap). Since the gaps are not symmetric under the considered  $\mathcal{S}$ -transformation, the corresponding blocks in the associated permutation matrix are diagonal (i.e., applying the identity to that part of the array), as seen in the insets of Fig. 4 (d); note that this yields  $q_{n; \nu}^{\pm} = j_{n; \nu}^{\pm} = 0$  in the gap in Fig. 4 (d,ii). The gaps may as well be locally symmetric under another transformation (e.g.  $\mathcal{P}$ -symmetric about their center), thus yielding a *nested* LS, which can be expressed through locally constant  $q_{n; \nu}^{\pm}$ ’s by accordingly modifying those permutation matrix blocks.

## B. Nonlocal currents in $\mathcal{PT}$ - and $\mathcal{KT}$ -symmetric non-Hermitian arrays

Having illustrated the various types of LS in terms of real modes in finite Hermitian arrays, we now demonstrate some properties of eigenmode NLCs for minimalistic examples of globally  $\mathcal{PT}$ - and  $\mathcal{KT}$ -symmetric non-Hermitian arrays, as shown in Fig. 5, and in particular their relation to spontaneous symmetry breaking. The nonhermiticity is here implemented by complex onsite potentials whose imaginary parts  $2\gamma_n$  represent loss ( $\gamma_n < 0$ ) or gain ( $\gamma_n > 0$ ) of density  $\rho_n$  in time, while the hoppings are taken to be real and equidirectional.

Global  $\mathcal{PT}$  symmetry, for which  $[\hat{H}, \hat{P}\hat{T}] = 0$ , is known to allow for parameter regimes of loss/gain elements  $\gamma_n$  where a subspace of common eigenstates  $|\phi^{\nu}\rangle$  of  $\hat{H}$  and  $\hat{P}\hat{T}$  with real  $\hat{H}$ -eigenvalues exists. The rest of  $\hat{H}$ -eigenstates are ‘spontaneously’ symmetry-broken, that is, non- $\hat{P}\hat{T}$ -eigenstates, but come in  $\hat{P}\hat{T}$ -related pairs  $|\phi^{\nu}\rangle, |\phi^{\nu'}\rangle$  with complex conjugate eigenvalues  $E_{\nu}, E'_{\nu}$ . If the whole discrete spectrum is real, then the system is said to be in a  $\mathcal{PT}$ -unbroken phase. The occurrence of  $\mathcal{PT}$ -unbroken modes can be seen as originating from the balance between loss and gain in density that a  $\hat{P}\hat{T}$ -symmetric  $\hat{H}$  enables: Since  $\rho_n$  in  $\hat{P}\hat{T}$  eigenstates is  $\mathcal{P}$ -symmetric, the gain on any site  $n$  is balanced by the loss at site  $\bar{n}$ , as seen from Eq. (14), and the current  $j_n$  flowing in the state keeps  $\rho_n$  stationary.

The  $\mathcal{PT}$ -unbroken modes are naturally distinguished by vanishing of the corresponding constant NLCs  $q_{n; \mathcal{P}}^{\pm}$ , as follows from Eq. (49) for the case  $\mathbb{D} = \mathbb{N}$  of global symmetry. This is illustrated in Fig. 5 (i) for a  $\mathcal{PT}$ -symmetric  $N = 5$ -site array with two loss/gain parameters  $\gamma, \eta$ , where a real central onsite energy  $v$  is added to break the  $\pm E_{\nu}^{\circ}$  symmetry of the  $\hat{H}$ -eigenvalues  $E_{\nu} = E_{\nu}^{\circ} + i\Gamma_{\nu}/2$  shown in Fig. 5 (a,i). As we see, all  $q_{\mathbb{N}; \nu}^{\pm}$  vanish within the  $\gamma$ -range (for fixed  $\eta$ ) corresponding

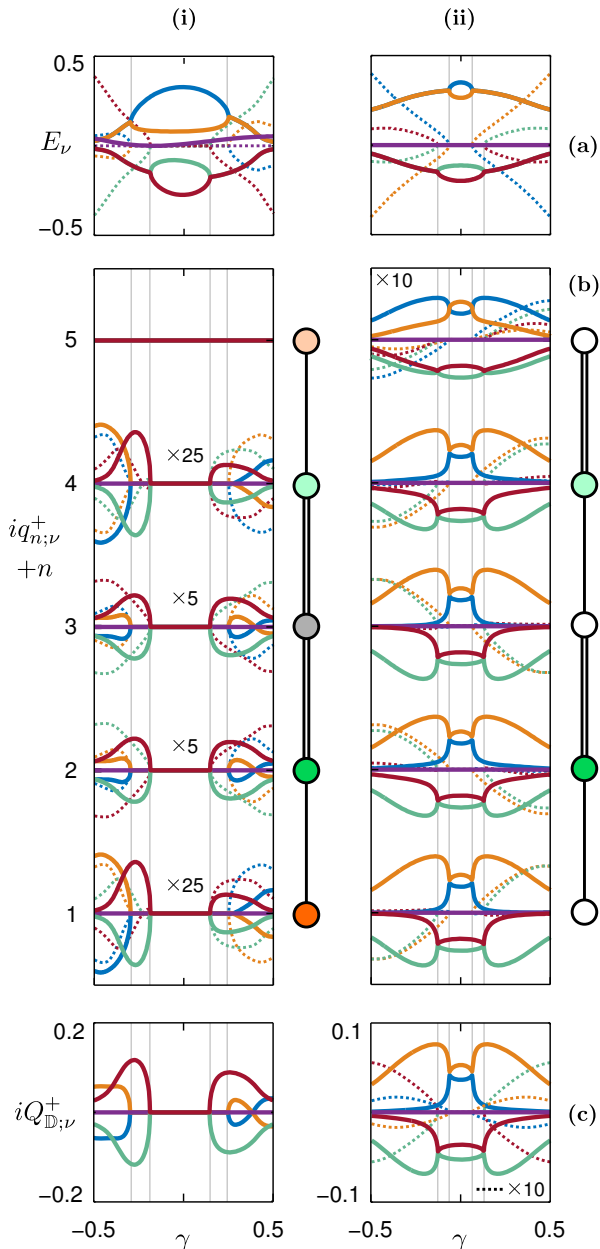


FIG. 5. Real (solid) and imaginary (dotted) part of (a) spectrum  $E_\nu$ , (b) spatially resolved upper NLCs  $i q_{n;\nu}^+$  (offset by site index  $n$ ), and (c) total upper NLC  $i Q_{\mathbb{D};\nu}^+$  within  $\mathbb{D}$ , in the modes  $\nu$  of a (i)  $\mathcal{PT}$ -symmetric array with  $\{v_n\} = \{i\eta, i\gamma, u, -i\gamma, -i\eta\}$ ,  $\{h_{n,n+1}\} = \{h, 2h, 2h, h\}$  where  $u = \eta = 0.06$  and  $h = 0.1$ , and a (ii)  $\mathcal{KT}$ -symmetric array with  $\{v_n\} = \{0, u + i\gamma, 0, u - i\gamma, 0\}$ ,  $\{h_{n,n+1}\} = \{h, 2h, h, 2h\}$  where  $u = 0.15$  and  $h = 0.1$ , for varying loss/gain parameter  $\gamma$ . Vertical lines indicate exceptional values of  $\gamma$  where transitions from complex to real eigenvalues  $E_\nu$  occur, corresponding to transitions from complex to (i) zero  $q_{n;\mathcal{P}}^+$  and (ii) imaginary  $q_{n;\mathcal{K}}^+$  in the respective modes. By convention,  $\mathbb{D} \equiv \{1, 2\}$  in (ii); see text.

to the unbroken phase of real  $E_\nu$  in Fig. 5(a.i). In the  $\mathcal{PT}$ -broken phase of complex  $E_\nu$ , the  $q_{n;\nu}^\pm$  are not spatially constant, since  $q_{n\mp 1;\nu}^\pm = q_{n;\nu}^\mp \neq q_{n;\nu}^\pm$  for  $\Gamma_\nu \neq 0$  (and  $\beta_n = 0$ ) in Eq. (38). Note here that  $q_{N;\mathcal{P}}^+ = 0$  and  $q_{1;\mathcal{P}}^- = 0$  identically in a finite array  $\mathbb{N}$  since they ‘flow’ on the nonexistent links  $(0, 1)$  and  $(N, N + 1)$ , respectively. While generally  $q_{n;\nu}^\pm \neq 0$  in the  $\mathcal{PT}$ -broken phase, the remnant of  $\mathcal{PT}$  symmetry in the occurrence of  $\mathcal{PT}$ -related eigenmode pairs is expressed by vanishing sum of NLCs: Since  $q_{n;\nu}^\pm$  in a  $\hat{H}$ -eigenstate  $|\phi^\nu\rangle$  is proportional to the difference of  $\phi_{n\pm 1}^{\nu*} h_{n,n\pm 1}^* \phi_{n;\nu}^\pm$  from its

$\mathcal{PT}$  image, it will be opposite  $q_{n;\nu'}^\pm$  in the paired eigenstate  $|\phi^{\nu'}\rangle = \hat{P}\hat{T}|\phi^\nu\rangle$  with  $E_{\nu'} = E_\nu^*$ ,

$$q_{n;\nu}^\pm + q_{n;\nu'}^\pm = 0. \quad (73)$$

Summing separately the  $q_{n;\nu}^\pm$  along the array, the total upper/lower link NLCs  $Q_{\mathbb{D};\nu}^\pm = \sum_{n \in \mathbb{D}} q_{n;\nu}^\pm$  (here  $\mathbb{D} = \mathbb{N}$ ) in state  $|\phi^\nu\rangle$  each serve as a single parameter which distinguish  $\mathcal{PT}$ -unbroken ( $Q_{\mathbb{D};\nu}^\pm = 0$ ) from  $\mathcal{PT}$ -broken ( $Q_{\mathbb{D};\nu}^\pm \neq 0$ ) modes for a given setup configuration. This is seen in Fig. 5(c.i) for  $Q_{\mathbb{D};\nu}^+$ . Note that the  $Q_{\mathbb{D};\nu}^\pm$  are imaginary due to Eq. (57) (left). Further, the remnant of  $\mathcal{PT}$  symmetry of the Hamiltonian in the broken phase may be expressed by the vanishing sum of  $Q_{\mathbb{D};\nu}^\pm$  over all modes,  $\sum_\nu Q_{\mathbb{D};\nu}^\pm = 0$ .

The nonlocal charge (quasipower)  $\Sigma_\psi^\mathbb{N} = \langle \psi | \hat{\Sigma} | \psi \rangle$  with  $\hat{\Sigma} = \hat{P}$  in the  $\mathcal{PT}$ -symmetric array for a general state  $|\psi\rangle$  remains constant in time (longitudinal direction)  $t$ , as mentioned in Sec. III C, in accordance with its vanishing total NLC,  $Q_\mathbb{N} = Q_\mathbb{N}^+ + Q_\mathbb{N}^- = 0$ . In particular, for the eigenmodes  $|\phi^\nu\rangle$  addressed here, we have

$$\Gamma_\nu \Sigma_\nu^\mathbb{N} = \partial_t \Sigma_\nu^\mathbb{N} = Q_{\mathbb{N};\nu} = 0, \quad (74)$$

which shows that the nonlocal charge  $\Sigma_\nu^\mathbb{N}$  is zero in  $\mathcal{PT}$ -broken eigenmodes with  $\Gamma_\nu \neq 0$ .

The  $\mathcal{PT}$  symmetry of  $\hat{H}$  is not a necessary condition for the occurrence of real  $E_\nu$  [54] and thereby invariant NLCs, of interest here. Indeed, real spectra may also occur in  $\mathcal{KT}$ -symmetric arrays of certain type, which we now exploit to show the induced invariance of translation NLCs  $q_{n;\mathcal{K}}^\pm$ . Specifically, we implement a non-Hermitian version of the Su-Schrieffer-Heeger model [55], which can be considered as a special case of the non-Hermitian Aubry-André-Harper model proposed in Ref. [56], in an array of odd size  $N$  where the hoppings are  $\mathcal{K}$ -symmetric with period  $L = 2$  and the potential is simultaneously  $\mathcal{KT}$ - and  $\mathcal{PT}$ -symmetric. The latter property enables the presence of loss/gain-balanced eigenmodes with real  $E_\nu$  [56]. Note that such an array is asymmetric under any cyclic shift permutation, that is, under action of an invertible matrix  $K_\mathbb{D}$ , since it does not consist of an integer number of periods. By convention we thereby set  $\mathbb{D} \equiv \{1, 2, \dots, N - L - 1\} = \{1, 2\}$ , the largest union of consecutive periods (starting from  $n = 1$ ) where  $H_{m,n} = H_{m+L,n+L}$ , and let  $K_\mathbb{D}$  be the  $L = 2$  cyclic shift matrix in Eq. (26b).

In Fig. 5(ii) the behavior of the  $q_{n;\mathcal{K}}^+$  is shown for the eigenmodes of a  $N = 5$ -site array with a single pair of sites with loss/gain parameter  $\gamma$  which supports a phase of real  $E_\nu$  in the eigenspectrum shown in Fig. 5(a.ii). Like in the  $\mathcal{PT}$ -symmetric case above, real onsite energies  $v$  are added to break the  $\pm E^\circ$ -symmetry of the spectrum. As we see in Fig. 5(b.ii), the  $\gamma$ -region with real  $E_\nu$  for each eigenmode is distinguished by a spatially constant and imaginary  $q_{n;\mathcal{K};\nu}^+$ , where  $-q_{n;\mathcal{K};\nu}^* = q_{n-L;\mathcal{K};\nu}^+$  is assigned to the last three sites  $\mathbb{N} \setminus \mathbb{D} = \{3, 4, 5\}$ ; see Eq. (59) and below. Outside this  $\gamma$ -region, the  $q_{n;\mathcal{K};\nu}^\pm$  vary along the array and have a real part, signifying the spontaneous breaking of loss/gain balance in the eigenstates. In analogy to the  $\mathcal{PT}$ -symmetric case above, though, a remnant of the symmetry of the system can be expressed in the broken phase by the imaginary sums  $\sum_\nu Q_{\mathbb{D};\nu}^\pm \in i\mathbb{R}$ , as anticipated by the  $Q_{\mathbb{D};\nu}^+$  shown in Fig. 5(c.ii). The characteristic of imaginary NLCs in the unbroken phase thus survives in the sum of total NLCs within  $\mathbb{D}$  over all modes.

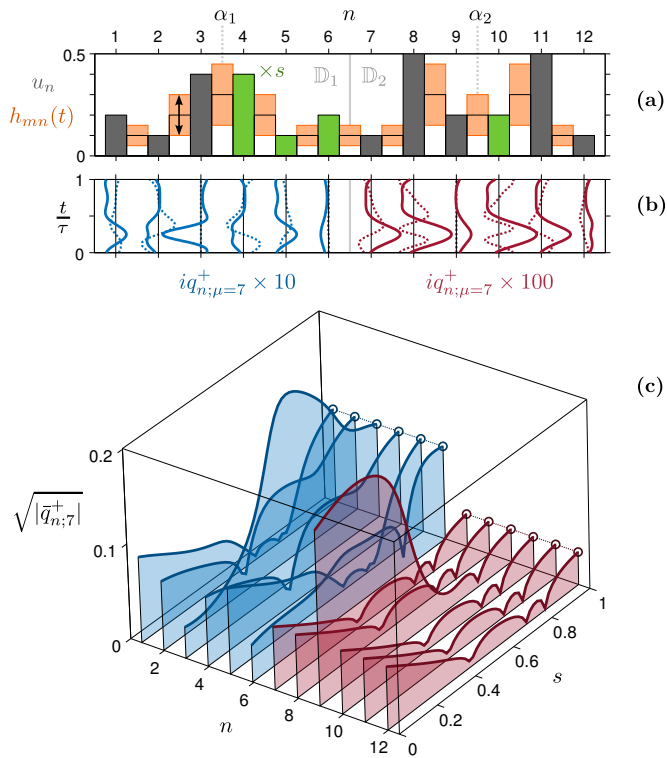


FIG. 6. (a) Setup with  $N = 12$  sites composed of two domains  $\mathbb{D}_1, \mathbb{D}_2$  which are locally  $\mathcal{P}$ -symmetric for the value  $s = 1$  of a scaling parameter  $s$  multiplying the onsite potentials  $u_3, u_4, u_5, u_{10}$  (colored green), with periodically modulated hoppings  $h_{n,n\pm 1}(t) = (1 + \frac{1}{2} \sin \pi t/8)h_{n,n\pm 1}(0)$ . (b) Time evolution over one period  $\tau$  of the NLC in Floquet mode  $\mu = 7$  associated with the local inversions  $\mathcal{P}_{\mathbb{D}_1}, \mathcal{P}_{\mathbb{D}_2}$ . (c) Period averaged NLC for varying scaling parameter  $s$ , showing the domainwise constancy in the case  $s = 1$  of local symmetry.

### C. Period invariants of bound Floquet states

In Sec. IV D it was shown how periodically modulated discrete systems reveal local spatial symmetries via the translation invariance of period-averaged NLCs  $\bar{q}_{n;\mu}^\pm$  in their quasistationary Floquet states. This applies generally for arbitrary boundary conditions and for both  $\mathcal{P}$  and  $\mathcal{K}$  spatial symmetry (or in combination with  $\mathcal{T}$ ). The counterpart of the  $\bar{q}_{n;\mu}^\pm$  in continuous systems was very recently shown to reliably expose defects in locally  $\mathcal{K}$ -symmetric potentials under periodic boundary conditions [57]. Here, the invariance of the period-averaged NLCs in  $\mathcal{P}$ -symmetric domains is demonstrated for bound Floquet states of discrete setups. In particular, we exploit the discrete tight-binding form of  $\hat{H}$  to drive the hoppings in time, corresponding to periodically modulated [58, 59] waveguide distances in the longitudinal direction of photonic arrays. Alternatively, one could drive the onsite potential [60], with an equivalent analysis in terms of NLCs.

We consider a Hermitian array of  $N = 12$  sites, whose local spatial symmetry is controlled by a scaling parameter  $s$  which multiplies the real potential  $u_n$  on sites  $n = 4, 5, 6, 10$ , as depicted in Fig. 6(a). For  $s = 1$  the setup has CLS, with the Hamiltonian elements of the setup dividing the array into two 6-site  $\mathcal{P}$ -symmetric subdomains  $\mathbb{D}_1$  and  $\mathbb{D}_2$  with inversion centers  $\alpha_1 = 3.5$  and  $\alpha_2 = 9.5$ , respectively, while for  $s \neq 1$  this LS is broken. Although any type of periodic driving is applicable, we here choose to add a simple in-phase harmonic modulation of relative amplitude  $f = 1/2$  to all hoppings around the (initial) equilibrium hopping strengths

$$h_{n,n\pm 1}^\circ = h_{n,n\pm 1}(t=0),$$

$$h_{n,n\pm 1}(t) = (1 + f \sin \omega t)h_{n,n\pm 1}^\circ; \quad n, n \pm 1 \in \mathbb{N}, \quad (75)$$

with frequency  $\omega = \pi/8$ . For a photonic waveguide array this would correspond to periodically curved waveguides such that the array cross section shrinks and expands homogeneously in the longitudinal direction.

The Floquet modes  $|\phi^\mu(t)\rangle$  of the system are computed with the Floquet matrix method [61] including a total of 6 sidebands (3 Fourier modes above and below the principal frequency  $\omega$ ). The upper NLC  $q_{n;\mu}^+(t)$  in the Floquet state with  $\mu = 7$  (chosen simply to yield distinctly varying NLCs) are shown in Fig. 6(b) for the CLS case  $s = 1$ . As is seen, at any instant  $t$  we have that  $i q_{n\mp 1;\mu}^\pm(t) = [i q_{n;\mu}^\pm(t)]^*$  in each  $\mathcal{P}$ -symmetric subdomain from Eq. (57) (left) which clearly holds also for the present dynamical NLCs. What is not directly anticipated from the time evolution of the NLCs is that their averages  $\bar{q}_{n;\mu}^\pm$  over a period  $\tau$  are real and spatially constant within  $\mathbb{D}_1$  and  $\mathbb{D}_2$ , as was established in Sec. IV D.

The profile of the period-averaged NLCs in relation to LS is illustrated in Fig. 6(c) by continuously varying  $s$ . For  $s < 1$  the system has no symmetry around  $\alpha_1$  in  $\mathbb{D}_1$ , and the  $|\bar{q}_{n \in \mathbb{D}_1;\mu}^+|$  are symmetric on the links around  $\alpha_1$ . The subdomain  $\mathbb{D}_2$ , where only one site is modified by  $s$ , has a gapped  $\mathcal{P}$  symmetry, and the  $|\bar{q}_{n \in \mathbb{D}_2;\mu}^+|$  are spatially constant in the subdomain  $\mathbb{D}_2 \setminus \{9, 10\}$  (i. e., only  $|\bar{q}_{9;\mu}^+| = |\bar{q}_{10;\mu}^+|$  on the central link across  $\alpha_2$  deviated from the rest). In both domains we see that  $|\bar{q}_{n;\mu}^+|$  becomes spatially constant in the limit of CLS when  $s = 1$ . Alternatively to the bound array considered here, an interesting perspective would be to study the behavior of NLCs in driven scattering setups where, e. g. Floquet bound states [62] may arise in the energy continuum.

## VI. NONLOCAL CURRENTS IN STATIONARY SCATTERING

In the previous section the NLCs and their invariance in LS domains, were investigated in various types of bound setups with discrete eigenspectra. We now apply the framework of NLCs to stationary scattering, where the energy  $E$  (longitudinal propagation constant for photonic waveguides) is a given input parameter, to demonstrate their domainwise invariance and relation to transmission in discrete structures with LSs.

To simulate scattering of an incident monochromatic wave on a localized potential in the discrete system, we attach semi-infinite chains with real constant onsite elements  $v_n = v$  and hoppings  $h_n^\pm = h$  on the left ( $n \leq 0$ ) and right ( $n \geq N + 1$ ) of the  $N$ -site scatterer. In the homogeneous chain leads, stationary solutions of the SE (2) are linear combinations of plain wave states  $|\pm\rangle e^{-iEt}$  where  $\langle n|\pm\rangle = e^{\pm ikn} \equiv \zeta^{\pm n}$  with quasimomentum  $k$  for energies obeying the dispersion relation

$$E = v + 2h \cos k. \quad (76)$$

For ‘biased’ setups with different lead Hamiltonians ( $v_{n < 1} \neq v_{n > N}$  and/or  $h_{n < 1}^\pm \neq h_{n > N}^\pm$ ) the plain wave states are flux normalized by the respective factor  $[h \sin k]^{1/2}$  with  $k$  given by the lead dispersion; we here consider unbiased setups with equal  $v, h$  in the two leads for simplicity. The spatial amplitudes  $a_n$  of a scattering state  $|\psi_E\rangle$  are expanded in the plain waves of the leads as ( $\zeta = e^{ik}$ )

$$a_n = \begin{cases} c_<^+ \zeta^{+n} + c_<^- \zeta^{-n}, & n < 1 \\ c_>^+ \zeta^{+n} + c_>^- \zeta^{-n}, & n > N \end{cases} \quad (77)$$

on the left and right of the scatterer, respectively. The computation of the amplitudes  $a_n$  along the scattering region as well as the output amplitudes  $c_{<}^{\pm}, c_{>}^{\pm}$  for given input is presented in compact form in Appendix A.

An incoming plain wave with unit amplitude from the left, setting  $c_{<}^+ = 1, c_{>}^+ = 0$  (from the right, setting  $c_{<}^+ = 0, c_{>}^+ = 1$ ), is reflected with amplitude  $c_{<}^- = \tau$  ( $c_{>}^+ = \tau'$ ) and transmitted with amplitude  $c_{>}^+ = t$  ( $c_{<}^- = t'$ ). These scattering amplitudes define the scattering matrix  $S$  which maps general input amplitudes to their output in the  $|\pm\rangle$  basis,

$$\begin{bmatrix} c_{<}^- \\ c_{>}^+ \end{bmatrix} = S \begin{bmatrix} c_{<}^+ \\ c_{>}^- \end{bmatrix}, \quad S = \begin{bmatrix} \tau & t' \\ t & \tau' \end{bmatrix}. \quad (78)$$

The reflection and transmission coefficients are given by  $\mathfrak{R} = |\tau|^2$  and  $\mathfrak{T} = |t|^2$ , respectively, with  $\mathfrak{R} + \mathfrak{T} = 1$  dictated by current conservation in the absence of (imbalanced) loss and gain.

In the following, we will focus on (local)  $\mathcal{P}$ -symmetric scatterers, whose corresponding NLCs are to be related to perfect transmission ( $\mathfrak{T} = 1$ ) of composite setups. The NLC on the first links on the left and right of a scatterer localized in a domain  $\mathbb{D}$  can generally be written in terms of the in- and outgoing amplitudes in the  $|\pm\rangle$  basis as

$$\begin{aligned} q_{l-1,l} &= q_{r+1,r}^* = 2h \sin k \left( \hat{c}_{<}^{+\ast} \hat{c}_{>}^- - \hat{c}_{<}^- \hat{c}_{>}^+ \right) \\ &= ih(\zeta^* - \zeta) \begin{bmatrix} \hat{c}_{<}^+ \\ \hat{c}_{>}^- \end{bmatrix}^\dagger A^\dagger \Lambda A \begin{bmatrix} \hat{c}_{>}^+ \\ \hat{c}_{<}^- \end{bmatrix} \end{aligned} \quad (79)$$

where  $\Lambda = \begin{bmatrix} 0 & 1 \\ -1 & 0 \end{bmatrix}$ ,  $\hat{c}_{<(>)}^{\pm} = \zeta^{\pm\alpha} c_{<(>)}^{\pm}$  correspond to a shift of the scatterer by  $-\alpha$  to the origin via the matrix  $A(\alpha) = d[\zeta^{+\alpha}, \zeta^{-\alpha}]$ , with the center  $\alpha$  of  $\mathbb{D}$  taken to coincide with the center of inversion (we suppress the subscript  $\mathcal{P}$  in  $q_{n;\mathcal{P}}^{\pm}$  from here on). Note that, since the scattering matrix  $S$  connects  $|\pm\rangle$ -amplitudes, the above expression for the NLC remains essentially the same for a continuous system: The discreteness of the system enters merely through the factor  $h(\zeta - \zeta^*) = 2ih \sin k$ , which is replaced by  $ik$  in the continuum limit (with real  $h$ ) where the NLC becomes a two-point quantity  $q(x, \bar{x})$ .

Substituting the outgoing amplitudes  $c_{<}^-, c_{>}^+$  from Eq. (78), the NLC above takes the form

$$\begin{aligned} q_{l-1,l} &= q_{r+1,r}^* = 2h \sin k \times \\ &\{ (1 - \hat{t}^* \hat{t}') \hat{c}_+^* \hat{c}_- - |t|^2 \hat{c}_+ \hat{c}_-^* - \hat{t}^* t |\hat{c}_+|^2 - t^* \hat{t}' |\hat{c}_-|^2 \}, \end{aligned} \quad (80)$$

where  $\hat{c}_+ \equiv \zeta^{+\alpha} c_{<}^+, \hat{c}_- \equiv \zeta^{-\alpha} c_{>}^-$  and  $\hat{t} \equiv \zeta^{-2\alpha} t$  are the ingoing and reflection amplitudes, respectively, for the same scatterer shifted to the origin ( $\alpha \rightarrow 0$ ), and where it was used that  $t = t'$  in general [63, 64] for nonsingular Hamiltonians.

### A. Local $\mathcal{P}$ -symmetry and perfect transmission

Let us now assume the scatterer to be  $\mathcal{P}$ -symmetric within a connected domain  $\mathbb{D}$  and Hermitian with equidirectional hoppings, meaning that  $q_{\mathbb{D}}^+ = q_{l-1,l} \in i\mathbb{R}$  is translation invariant along  $\mathbb{D}$ . We then also have that  $\hat{t} = \hat{t}'$  from the  $\mathcal{P}$  symmetry of the scatterer (around the origin) and  $1 - |\tau|^2 = |t|^2$ ,  $t^* \hat{t}' = -\hat{t}^* t$  from the S-matrix unitarity, so that the NLC expression reduces to

$$\begin{aligned} q_{\mathbb{D}}^+ &= q_{\mathbb{D}}^{-\ast} = 2h \sin k \times \\ &\{ |t|^2 (\hat{c}_+^* \hat{c}_- - \hat{c}_+ \hat{c}_-^*) - \hat{t}^* t (|\hat{c}_+|^2 - |\hat{c}_-|^2) \}, \end{aligned} \quad (81)$$

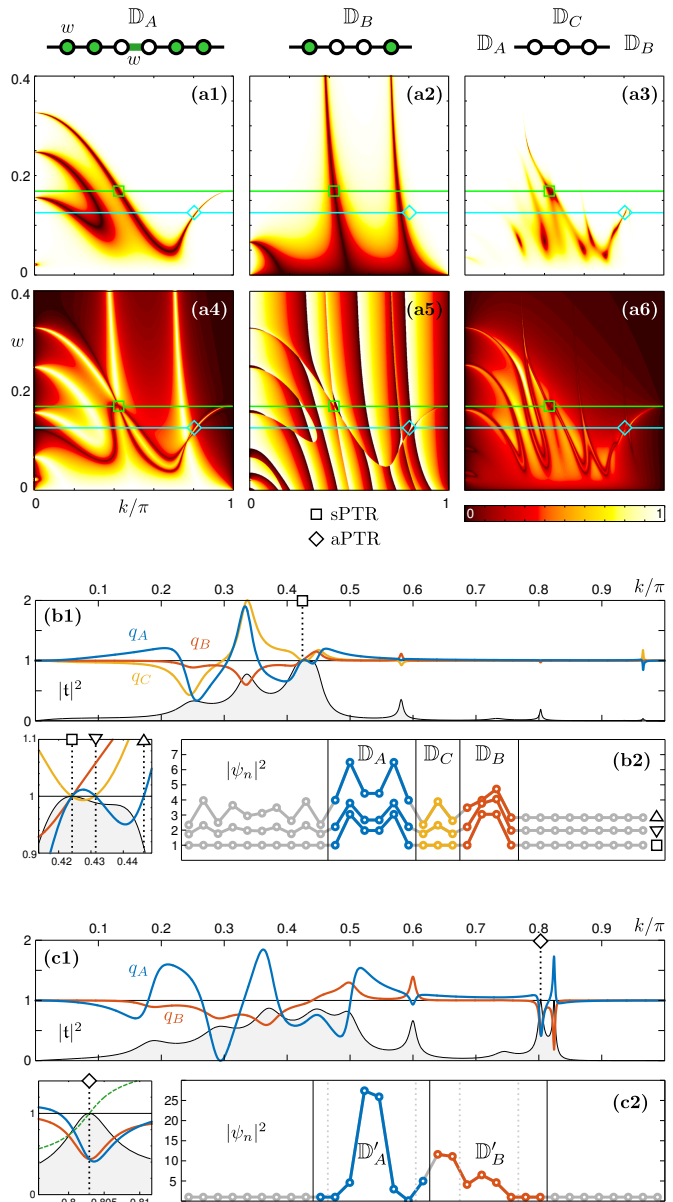


FIG. 7. Scattering off a locally  $\mathcal{P}$ -symmetric Hermitian array composed of three LS domains:  $\mathbb{D}_A$  and  $\mathbb{D}_B$  each containing a scatterer with Hamiltonian parameter  $w$  (top sketch), and an intervening free propagation domain  $\mathbb{D}_C$ . Reflection magnitudes **(a1)**  $|r_A|$  of  $\mathbb{D}_A$ , **(a2)**  $|r_B|$  of  $\mathbb{D}_B$ , and **(a3)**  $|t|$  of the composite array  $\mathbb{D} = \{\mathbb{D}_A, \mathbb{D}_C, \mathbb{D}_B\}$ , as well as quantities **(a4)**  $|q_A| - |r_A|^{1/2}$ , **(a5)**  $|(\arg \tau'_A - \arg \tau'_B) \bmod 2\pi|/2\pi$ , and **(a6)**  $||q_A| - |q_B||^{1/2}$ , which vanish at unit transmission (PTR,  $\tau = 0$ ), for varying  $w$  and  $k$ . An sPTR (aPTR) occurs at  $w, k$  where  $\tau'_A = \tau'_B = 0$  ( $\neq 0$ ), in which case  $|q_A| = |q_B| = 0$  ( $\neq 0$ ), indicated by  $\square$  ( $\diamond$ ). **(b1)** Transmission  $|t|^2$  and NLCs  $q_{A,B,C}$  (offset by 1 and scaled by overall maximum) in varying  $k$  for  $w \approx 0.1687$  and **(b2)** density  $|\psi_n|^2$  (offset by 1, 2, 3) at  $k$ -values indicated by  $\square, \triangle, \nabla$  in zoomed inset of **(b1)** where  $q_A = q_B = q_C = 0$  (corresponding to the sPTR in **(a)**),  $q_A = 0 \approx q_C, q_A = 0$ , respectively.  $|\psi_n|^2$  is  $\mathcal{P}_{\mathbb{D}_X}$ -symmetric when  $q_X = 0$  ( $X = A, B, C$ ). **(c1)**  $|t|^2$  and  $q_{A,B}$  for  $w \approx 0.1254$  and **(c2)**  $|\psi_n|^2$  at  $k$  indicated by  $\diamond$  in inset where  $q_A = q_B \neq 0$  corresponding to the aPTR in **(a)**; green dashed line shows  $\arg\{t\zeta^{2(\alpha_2 - \alpha_1)}\}/\pi$ .  $\mathbb{D}_A$  ( $\mathbb{D}_B$ ) is here augmented symmetrically by 1 (2) site(s) into  $\mathbb{D}'_A$  ( $\mathbb{D}'_B$ ).

where we note that  $\hat{t}^* t \in i\mathbb{R}$ . This expression shows how the  $q_{\mathbb{D}}^{\pm}$  depend on the characteristics  $t, \tau$  and position  $\alpha$  of the scatterer (domain  $\mathbb{D}$ ) as well as the amplitudes incident on it.

At the center  $k = 0$  and edges  $k = \pm\pi$  of the leads'

Brillouin zone, the scattering NLCs vanish generically. Away from those  $k$ -points,  $q_{\mathbb{D}}^{\pm} = 0$  and thereby symmetric density  $\rho_n$  in  $\mathbb{D}$  (see Eq. (49)) can be achieved by tuning the ingoing amplitudes to satisfy  $(|\hat{c}_+|^2 - |\hat{c}_-|^2) / \text{Im}[\hat{c}_+^* \hat{c}_-] = \pm 2|t|/|\tau|$  for  $\hat{\mathbf{t}}^* \hat{\mathbf{t}} \in i\mathbb{R}^{\pm}$ . For example, this is satisfied for  $\hat{c}_+ = 1$  and  $|\hat{c}_-| = \sqrt{2} - 1$  at all  $E$  where  $\arg \hat{c}_- = \pm \arcsin |\tau/t|$ . A special situation occurs for  $S$ -matrix eigenstates, in which  $\hat{c}_+ = \pm \hat{c}_-$  and thus  $q_{\mathbb{D}}^{\pm} = 0$  for any  $\hat{\mathbf{t}}, \hat{\mathbf{t}}$ . For a globally  $\mathcal{P}$ -symmetric (about  $\alpha = 0$ ) Hermitian scatterer, those states are simultaneously  $\hat{P}$  eigenstates with eigenvalues  $\lambda_{\mathcal{P}} = \pm 1$  and  $\hat{P}\hat{T}$  eigenstates with eigenvalues  $\lambda_{\mathcal{PT}} = e^{i\vartheta_\lambda}$  where  $\vartheta_\lambda = -2 \arg(c) - \arg(\hat{\mathbf{t}} \pm \hat{\mathbf{t}})$  (note that  $|\hat{\mathbf{t}} \pm \hat{\mathbf{t}}| = 1$  in this case).

In the most common setting for a single scatterer, however, there is only one incoming wave from the left ( $\hat{c}_- = 0$ ) or from the right ( $\hat{c}_+ = 0$ ). In this case,  $q_{\mathbb{D}}^{\pm} = 0$  if and only if the scatterer is transparent at the given  $k$ ,  $\tau = 0$  (or if  $t = 0$ , which strictly only occurs for singular potentials in unbiased 1D systems, in contrast to Fano transmission zeros when multiple interference paths are available [65]). Thus, perfect transmission  $\mathfrak{T} = 1$  is accompanied by a  $\mathcal{P}_{\mathbb{D}}$ -symmetric density  $\rho_n$  within  $\mathbb{D}$  ( $\mathcal{P}_{\mathbb{D}}\mathcal{T}$ -symmetric  $\psi_{n;E}$  up to a phase). The assumption  $\hat{c}_{-(+)} = 0$  for left (right) incidence is compatible with the connection to another, generally different, locally symmetric scatterer on the right (left) of  $\mathbb{D}$  which is also transparent at the same  $k$ . By adjusting the Hamiltonian parameters, a CLS setups may be assembled from multiple, simultaneously transparent scatterers in LS domains  $\mathbb{D}_d$  ( $d = 1, 2, \dots$ ), with the state density following the LS of the setup. We refer to such a state as a ‘symmetric’ perfect transmission resonance (sPTR); an example is illustrated in Fig. 7. We here have two scatterers localized in domains  $\mathbb{D}_A$  and  $\mathbb{D}_B$ , connected via a free (with  $h, u$  like in the leads) gap  $\mathbb{D}_C$ . As we see in Fig. 7 (b), the vanishing of the individual  $q_A^+, q_B^+, q_C^+$  reveals the  $k$  at which the density  $\rho_n$  is locally symmetric in  $\mathbb{D}_A, \mathbb{D}_B, \mathbb{D}_C$ , respectively, and an sPTR occurs when  $q_A^+ = q_B^+ = q_C^+ = 0$ .

In contrast to an sPTR, transparency ( $\mathfrak{T} = 1$ ) may also occur in a state whose density does not follow any LS of the setup, which we refer to as an ‘asymmetric’ PTR (aPTR). To see the relation of the NLCs to the occurrence of an aPTR, we consider a Hermitian setup of two different scatterers  $\mathbb{D}_1$  and  $\mathbb{D}_2$  with corresponding scattering matrices  $S_1$  and  $S_2$ . The total  $S$ -matrix has elements  $\tau = \tau_1 + \mathfrak{p}t_1' \tau_2 t_1$ ,  $\tau' = \tau_2' + \mathfrak{p}t_2 \tau_1' t_2'$ , and  $t = t' = \mathfrak{p}t_1 t_2$ , where  $\mathfrak{p} = (1 - \tau_2 \tau_1')$  accounts for all orders of multiple reflections between the scatterers. The condition  $|t| = 1$  for a PTR leads to  $|\tau_1' - \tau_2|^2 = -4|\tau_1'| |\tau_2| \sin \vartheta_1' \sin \vartheta_2$ , with  $\vartheta_{1,2}^{(i)}$  being the phases of  $\tau_{1,2}^{(i)}$ , which in turn is equivalent to

$$\tau_1' = \tau_2^*, \quad (82)$$

as can be seen geometrically in the complex plane. Thus, in the special case  $|t_1| = |t_2| = 1$ , the phases  $\vartheta_1', \vartheta_2$  are arbitrary, while  $(\vartheta_1' + \vartheta_2) \bmod 2\pi = 0$  must hold for  $|t_1| = |t_2| \neq 1$  [19]. If both scatterers are  $\mathcal{P}$ -symmetric about their centers, it additionally holds that  $\hat{\mathbf{t}}_d^* \hat{\mathbf{t}}_d \in i\mathbb{R}$  ( $d = 1, 2$ ), and it can then be shown that

$$t = \pm \zeta^{2(\alpha_1 - \alpha_2)} \quad (83)$$

at the PTR. That is, the phase of the transmission amplitude depends (up to  $\pi$ ) only on the distance between the centers of any two arbitrary but locally  $\mathcal{P}$ -symmetric scatterers.

Assuming the scatterers to be  $\mathcal{P}$ -symmetric, each will also have spatially constant NLC  $q_{\mathbb{D}_d}^{\pm} \in i\mathbb{R}$  ( $d = 1, 2$ ) at a given

$E$ . Using the general expression (79), the NLCs in  $\mathbb{D}_1$  can be written as

$$q_{\mathbb{D}_1}^+ = -q_{\mathbb{D}_1}^- = ih(\zeta^* - \zeta) \times \begin{bmatrix} c_+ \\ \tau c_+ \end{bmatrix}^\dagger A^\dagger \Lambda A C \begin{bmatrix} c_+ \\ c_- \end{bmatrix}, \quad C = \mathfrak{p} \begin{bmatrix} t_1 & \tau_1' t_2' \\ \tau_2 t_1 & t_2' \end{bmatrix}, \quad (84)$$

in terms of the global in- and outgoing  $|\pm\rangle$ -amplitudes  $c_+ = c_+^<, c_- = c_-^>$ , where the ‘connection’ matrix  $C$  was used to eliminate the amplitudes between the scatterers (note that the  $\mathbb{D}_1$  and  $\mathbb{D}_2$  may be directly attached in the above formulation). Considering now the case of a PTR ( $\tau = 0, \tau_1' = \tau_2^*$ ) under left incidence only ( $c_-^> = 0$ ), the upper NLC becomes

$$q_{\mathbb{D}_1}^+ = \pm 2ih \sin k \frac{|t_1|}{|t_1|} |c_+|^2. \quad (85)$$

On the other hand, its difference from  $q_{\mathbb{D}_2}^+$  is generally given by

$$q_{\mathbb{D}_1}^+ - q_{\mathbb{D}_2}^+ = ih(\zeta^* - \zeta) \times \mathfrak{p} t_1 \left\{ \left(1 - \tau^* \zeta^{2(\alpha_1 - \alpha_2)}\right) \zeta^{-2\alpha_1} \tau_2 - \zeta^{2\alpha_1} \tau^* \right\} |c_+|^2 \quad (86)$$

for left incidence. In the case of a PTR, applying conditions (82) and (83) makes Eq. (86) consistent with Eq. (84) only if

$$q_{\mathbb{D}_1}^+ = \pm q_{\mathbb{D}_2}^+, \quad (87)$$

for  $\hat{\mathbf{t}}_d^* \hat{\mathbf{t}}_d \in i\mathbb{R}^{\pm}$ , the sign being determined by the details of a given setup. This is demonstrated in the example setup of Fig. 7 (c), featuring an aPTR where the nonzero NLCs  $q_{\mathbb{D}_1}^+ \equiv q_A^+$  and  $q_{\mathbb{D}_2}^+ \equiv q_B^+$  cross.

The relation between NLCs and transparency of a two-scatterer setup can be verified for a setup with a gap of two ‘free’ sites  $c-1, c$  ( $v_{c-1} = v_c = v, h_{c-1,c} = h$ ) between  $\mathbb{D}_1$  and  $\mathbb{D}_2$ , for which an explicit calculation yields

$$q_{\mathbb{D}_1}^+ = t \zeta^{2(\alpha_2 - \alpha_1)} q_{\mathbb{D}_2}^+ \quad (88)$$

for  $|t| = 1$ . Since the  $q_{\mathbb{D}_1}^+ \equiv q_{l-1; \mathcal{P}_{\mathbb{D}_1}}^+, q_{\mathbb{D}_2}^+ \equiv q_{r; \mathcal{P}_{\mathbb{D}_2}}^+$  are constant and imaginary, we have that  $t \zeta^{2(\alpha_2 - \alpha_1)} = \pm 1$ , in accordance with Eq. (83).

To summarize, when the setup of two LS scatterers is perfectly transmitting, then it always holds that  $|q_{\mathbb{D}_1}^+| = |q_{\mathbb{D}_2}^+|$ , with two possible cases with respect to the symmetry of  $\rho_n$ : (i) If  $|q_{\mathbb{D}_1}^+| = |q_{\mathbb{D}_2}^+| = 0$ , then we have an sPTR with  $\rho_n$  being  $\mathcal{P}$ -symmetric in the LS domains. (ii) If  $|q_{\mathbb{D}_1}^+| = |q_{\mathbb{D}_2}^+| \neq 0$ , then we have an aPTR and  $\rho_n$  is asymmetric with respect to the LS domains. The NLCs thus connect the transport properties of globally asymmetric systems to the spatially resolved profile of the scattering state amplitude with respect to its possible LSs. In composite CLS setup of multiple scatterers, there may be parts of locally symmetric and asymmetric  $\rho_n$  at a PTR indicated by zero and nonzero equal NLC invariants, respectively.

## B. Invariants in locally $\mathcal{PT}$ -symmetric scattering

We close this section by addressing the NLCs of scattering states in non-Hermitian setups. Since the energy is here a free input parameter which is chosen real, the translation invariance of the NLCs in locally  $\mathcal{PT}$ -symmetric domains is

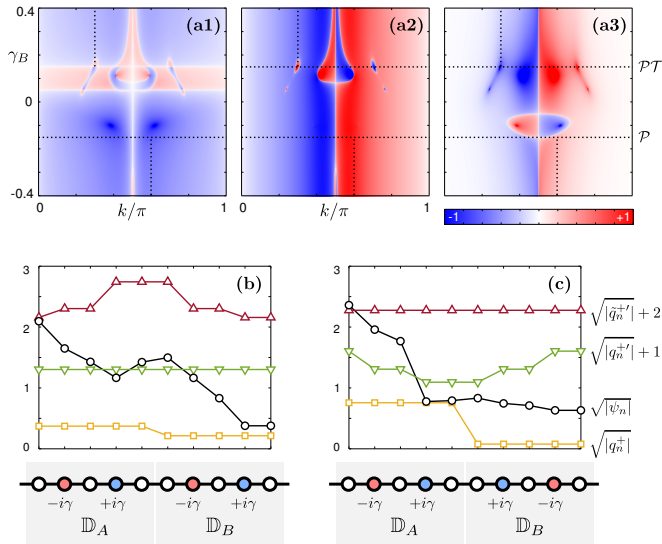


FIG. 8. Scattering off a locally  $\mathcal{PT}$ -symmetric non-Hermitian array  $\mathbb{D} = \{\mathbb{D}_A, \mathbb{D}_B\}$  with onsite elements  $\{v_n\}_X = \{0, -i\gamma_X, 0, +i\gamma_X, 0\}$  ( $X = A, B$ ) and common hoppings  $\{h_{n,n+1}\} = 0.1 \times \{1.0, 1.5, 1.5, 1.0\}$ . **(a1)** Quantity  $|\mathfrak{S}-1| - \sqrt{\Re\mathfrak{R}^*}$  of  $\mathbb{D}$  and NLCs **(a2)**  $q_A^+/i$  of  $\mathbb{D}_A$  and **(a3)**  $q_B^+/i$  of  $\mathbb{D}_B$  for unit incoming amplitude from the left, in varying  $k$  and  $\gamma_B$  for fixed  $\gamma_A = 0.15$ . The colormap is normalized to 1 in (a1) and truncated at  $\pm 1$  in (a2,a3); it scales with the power of 1/4 to increase contrast. **(b)** Density  $|\psi_n|^2$  (o) and spatially resolved NLCs  $q_n^+$  (□) for local  $\mathcal{P}_{\mathbb{D}_{A,B}}$  transforms,  $q_n^{+'}$  (▽) and  $\hat{q}_n^{+'}$  (△) for global  $\mathcal{P}$  transform, for  $\gamma_B = \gamma_A \equiv \gamma$  (global  $\mathcal{PT}$  symmetry) at  $k = \pi/3$  indicated by upper dotted line in (a1). **(c)** Same as (b) but for  $\gamma_B = -\gamma_A \equiv \gamma$  (global  $\mathcal{P}$  symmetry) at  $k = 0.6\pi$  indicated by lower dotted line in (a1).

manifest for any choice of loss/gain parameters. In the case of a  $\mathcal{PT}$ -symmetric scatterer, the S matrix elements are subject to the generalized unitarity relation [64]

$$|t|^2 - \frac{t^*}{t} \hat{t} \hat{t}' = 1 \Rightarrow |\mathfrak{S} - 1| = \sqrt{\Re\mathfrak{R}^*} \quad (89)$$

for  $t \neq 0$ , with  $t^* \hat{t}, \hat{t}^* \hat{t}' \in i\mathbb{R}$ . The general expression (80) for the NLC then becomes

$$q_{\mathbb{D}}^+ = q_{\mathbb{D}}^{-*} = 2h \sin k \times \left\{ |t|^2 (\hat{c}_+^* \hat{c}_- - \hat{c}_+ \hat{c}_-^*) - \hat{t}^* \hat{t} |\hat{c}_+|^2 - \hat{t}' \hat{t}^* |\hat{c}_-|^2 \right\}, \quad (90)$$

which further reduces to Eq. (81) if the  $\mathcal{PT}$ -symmetric scatterer is also Hermitian. A  $\mathcal{PT}$ -unbroken phase for a globally  $\mathcal{PT}$ -symmetric, two-terminal scattering setup may be identified as the parametric region of  $\hat{H}$  with unimodular S-matrix eigenvalues  $\lambda_S^{1,2}$  at given energy [39]. Indeed, for S-matrix eigenstates, where  $\hat{c}_{<(>)}^{-(+)} = \lambda_S^{1,2} \hat{c}_{<(>)}^{+(-)}$ , the NLC of Eq. (79) becomes

$$q_{\mathbb{D}}^+ = q_{\mathbb{D}}^{-*} = 2h \sin k \hat{c}_<^{+*} \hat{c}_>^- \left( 1 - |\lambda_S^{1,2}|^2 \right), \quad (91)$$

yielding a  $\hat{P}\hat{T}$  eigenstate when  $|\lambda_S^{1,2}| = 1$  since then  $q_{\mathbb{D}}^{\pm} = 0$ . The latter condition, however, can be met in Eq. (90) also for non-S-matrix eigenstates in dependence of the incoming amplitudes  $\hat{c}_<^{\pm}, \hat{c}_>^{\pm}$  for a given  $S(E)$ . The crossing from zero to nonzero NLC thus provides an extended identification of a  $\mathcal{PT}$  ‘phase transition’ in scattering beyond S-matrix eigenstates [28], identical to that of bound systems (as discussed above in Sec. VB).

More importantly, the vanishing of NLCs can be employed to identify configurations with *locally*  $\mathcal{PT}$ -invariant states, that is, where Eq. (49) is fulfilled in a  $\mathcal{PT}$ -symmetric subdomain of the setup. As an example, in Fig. 8 we consider a non-Hermitian setup of two attached domains  $\mathbb{D}_A, \mathbb{D}_B$  with loss/gain parameter pairs  $\pm\gamma_A, \pm\gamma_B$ , respectively. The setup is designed such that it is globally  $\mathcal{PT}$ -symmetric ( $\mathcal{P}$ -symmetric) for  $\gamma_B = \gamma_A$  ( $\gamma_B = -\gamma_A$ ). As we see in Fig. 8 (a1), there are values of  $\gamma_B \neq \gamma_A$  where Eq. (89) is fulfilled at certain energies (see white contours), such that the system behaves as being  $\mathcal{PT}$ -symmetric in terms of its S-matrix. Interestingly, it is possible to fulfill Eq. (89) at all  $k$  with a locally  $\mathcal{PT}$ -symmetric setup for appropriately chosen loss/gain parameters, as seen for the present setup for  $\gamma_B = \gamma_A/3 = 0.05$  (lower horizontal white line in Fig. 8 (a1)). In Fig. 8 (a2) and (a3) we see that the NLCs  $q_A^+$  and  $q_B^+$ , corresponding to local  $\mathcal{PT}$ -symmetry in  $\mathbb{D}_A$  and  $\mathbb{D}_B$ , vanish at different contours in the  $(k, \gamma_B)$ -plane, revealing the occurrence of locally symmetric density embedded into the globally  $\mathcal{PT}$ -asymmetric system.

Leaving a more comprehensive investigation of NLCs in relation to scattering properties of locally  $\mathcal{PT}$ -symmetric setups for future work, we focus now on their spatial constancy in 1D domains. This is illustrated in Fig. 8 (b) and (c), where the considered setup is, apart from locally  $\mathcal{PT}$ -symmetric, also globally  $\mathcal{PT}$ - and  $\mathcal{P}$ -symmetric, respectively. At the chosen generic  $k$ -values, the density profile  $|\psi_n|^2$  is completely asymmetric under any of those symmetry transformations at the chosen (generic)  $k$ -values. For the local  $\mathcal{P}$  transforms in  $\mathbb{D}_A$  and  $\mathbb{D}_B$ , the domainwise constancy of the associated NLC  $q_n^+$  reveals the local  $\mathcal{PT}$  symmetry of  $\hat{H}$  encoded in the scattering state. Note that this is achievable because  $E$  is set real as an input parameter, in contrast to non-Hermitian *bound* 1D systems where local  $\mathcal{PT}$  symmetry typically does not support real eigenenergies. In Fig. 8 (b), the constant NLC  $q_n^{+'}$  associated with global  $\mathcal{P}$  reflects the global  $\mathcal{PT}$  symmetry, while the alternative quantity  $\hat{q}_n^{+'}$  is symmetric; see Eq. (57). In Fig. 8 (c), we have the opposite situation:  $q_n^{+'}$  is symmetric, while the constant  $\hat{q}_n^{+'}$  reflects the global  $\mathcal{P}$  symmetry, even in the presence of loss and gain.

## VII. CONCLUSIONS AND PERSPECTIVES

A discrete nonlocal current-density continuity formalism was developed to relate localized spatial symmetries to Schrödinger wave properties in Hermitian and non-Hermitian lattice systems. Sources and sinks of the nonlocal currents (NLCs) are identified in the breaking of the local symmetries (LSs), with the associated charge evolution governed by the NLCs at symmetry domain boundaries. For stationary states, the symmetry-adapted NLCs are translationally invariant in one-dimensional finite domains with  $\mathcal{S}(\mathcal{T})$ -symmetric sub-Hamiltonians, where  $\mathcal{S} = \mathcal{P}$  (inversion) or  $\mathcal{K}$  (translation) is potentially combined with  $\mathcal{T}$  (time reversal). These invariant NLCs reflect the local symmetries of generic single-particle lattice Hamiltonians encoded into arbitrarily irregular field profiles, and enable the mapping between wave amplitudes of symmetry-related sites in finite domains. We illustrated the NLC invariance in cases of complete, overlapping, and gapped domainwise symmetry, as well as for non-Hermitian (locally)  $\mathcal{PT}$ - and  $\mathcal{KT}$ -symmetric (scattering) systems with balanced gain and loss. In scattering setups, the NLCs were further shown to classify perfect transmission resonances with respect to their spatially resolved density profile, being sym-

metric (asymmetric) in adjacent locally symmetric lattice subdomains with equal and zero (nonzero) NLC magnitude. Further, in periodically driven setups the NLC invariance was shown to be retained for quasi-stationary (Floquet) states on period-average, thus revealing LSs also far from equilibrium.

We have here utilized photonic waveguide arrays as an applicational platform since they are well described by a discrete Schrödinger equation with nearest neighbor couplings. The formalism and general results apply equally to other lattice systems modeled effectively by a discrete Schrödinger equation, like superlattice nanostructures or quantum dot arrays [18]. For stationary states the applicability is further broadened to generic wave mechanical systems described by a discretized Helmholtz equation, such as e. g. granular acoustic media with domainwise homogeneities [66]. In the limit of large site density with constant inter-site hopping, the same formalism can be equally employed for spatially continuous systems (with the lattice used as a numerical grid), treating simulations of, e. g., photonic multilayer devices [19, 20] or acoustic waveguides [21, 22].

The present operator formulation of the NLCs, expressed in Eq. (23), further enables a straightforward extension beyond nearest neighbor couplings or to higher dimensions, simply by including the additional couplings into the hopping operators  $\hat{H}^\pm$  accordingly. In general, the net NLC assigned to a site with (multidimensional) index  $\mathbf{n}$  will then consist of the sum of nonlocal link currents  $iq_{nm}^S = \psi_{\mathbf{n}}^* h_{S(\mathbf{n},\mathbf{m})} \psi_{S(\mathbf{m})} - \psi_{S(\mathbf{n})} h_{\mathbf{n},\mathbf{m}}^* \psi_{\mathbf{m}}^*$  over connected sites  $\mathbf{m}$  for a given symmetry operation  $S$ , defined in analogy with the 1D NLCs in Eq. (21). A thorough account on symmetry considerations and associated NLCs in planar discrete systems, where rotations and plane reflections add to the possible  $S$ -transforms, will be presented in a future work [67]. Multidimensional divergence naturally prevents individual  $q_{nm}^S$  from being spatially constant along a selected dimension, just as is the case for the usual current. NLC invariance does apply if the sites  $\mathbf{m}$  above represent next-nearest or (selected) remote neighbors along a *single* dimension, as is effectively the case, e. g., for zigzag chains with embedded scatterers [68] or discrete helical structures [69], respectively. Extended locally symmetric domains in such setups will then be distinguished by constant NLCs in arbitrary stationary states. Finally, the domainwise invariant stationary NLCs may be generalized to discrete interacting systems where the *interaction* itself is represented by a locally  $ST$ -symmetric function on the lattice sites. A promising case would be the discrete version of self-induced  $\mathcal{PT}$ -symmetric potentials [35, 52] in lattice subdomains, with the mean-field nonlinear (Gross-Pitaevskii) term  $\rho_n = |\psi_n|^2$  replaced by the nonlocal density  $\sigma_n = \psi_n^* \psi_{\bar{n}}$ . With the above perspectives, we believe that the developed connection between discrete nonlocal continuity and symmetry-induced subdomain invariants may contribute to the understanding of wave structure and response in discrete systems with localized spatial regularities.

## ACKNOWLEDGEMENTS

We are thankful to Malte Röntgen for fruitful suggestions and critical reading of the manuscript, as well as to Stefan Weimann and Alexandra V. Zampetaki for helpful discussions.

## Appendix A: Computation of scattering state for arbitrary input and scatterer type

Augmenting the scatterer domain  $\mathbb{N}$  by two lead sites on each side ( $n = -1, 0$  and  $n = N + 1, N + 2$  in the present indexing), we can solve the close-coupling equations (37) for the outgoing plane wave amplitudes  $c_{<}^-, c_{>}^+$  as well as the site amplitudes

$$\mathbf{a} \equiv [a_1, a_2, \dots, a_N]^\top \quad (\text{A1})$$

along the scatterer by sparse matrix multiplication and inversion of size  $N + 2$ . Specifically, using the asymptotic ansatz (77) for the two sites on either side of  $\mathbb{N}$ , we rearrange the Schrödinger system of  $N + 2$  next-neighbor equations to solve for  $c_{<}^-, c_{>}^+$  and  $\mathbf{a}$  in the form of the column vector

$$\begin{bmatrix} c_{<}^- \\ \mathbf{a} \\ c_{>}^+ \end{bmatrix} = -[WZ]^{-1} \begin{bmatrix} (h^* \zeta^* + \tilde{v}) \zeta^{+l} c_{<}^+ \\ \zeta_{<}^- \\ (h^* \zeta^* + \tilde{v}) \zeta^{-r} c_{>}^- \end{bmatrix}. \quad (\text{A2})$$

Here,  $l$  ( $r$ ) is the index of the lead site attached to the leftmost (rightmost) scatterer site,  $\tilde{v} = v - E$ , and

$$\zeta_{<}^- = \begin{bmatrix} h^* \zeta^{+l} c_{<}^+ \\ \mathbf{0}_{N-2} \\ h^* \zeta^{-r} c_{>}^- \end{bmatrix}, \quad Z = \begin{bmatrix} \zeta^{-l+1} & \mathbf{0}_N^\top & 0 \\ \zeta^{-l} & \mathbf{0}_N^\top & 0 \\ \mathbf{0}_N & I_N & \mathbf{0}_N \\ 0 & \mathbf{0}_N^\top & \zeta^r \\ 0 & \mathbf{0}_N^\top & \zeta^{r+1} \end{bmatrix}, \quad (\text{A3})$$

with  $\mathbf{0}_N$  being a  $1 \times N$  row vector of zeros and  $I_N$  the  $N \times N$  unit matrix. The  $(N + 2) \times (N + 4)$  matrix  $W$  is the  $(N + 2) \times (N + 2)$  block of  $H - EI$  corresponding to the domain  $\{l, \mathbb{N}, r\}$ , augmented by the column  $[h \ 0 \ \dots \ 0]^\top$  on the left and  $[0 \ \dots \ 0 \ h]^\top$  on the right.

With the scatterer domain defined as  $\mathbb{N} = \{1, 2, \dots, N\}$  we here have  $l = 0$  and  $r = N + 1$ . In the case  $N = 1$  of a single site scatterer,  $\zeta_{<}^-$  reduces to a single element

$$\zeta_{<}^- = h^* (\zeta^{+l} c_{<}^+ + \zeta^{-r} c_{>}^-). \quad (\text{A4})$$

Note also that for biased setups, the  $\tilde{v}$ ,  $h$  and  $k$  entering the top (bottom) row elements in Eq. (A2) are accordingly replaced by those of the left (right) lead; in the present work we consider unbiased setups.

The above method is essentially equivalent to propagating the input signal via the resolvent (lattice Green function) of the effective lead-coupled Hamiltonian of the scattering region. Here, however, we explicitly solve outgoing  $|\pm\rangle$ -amplitudes and combine them compactly into a column vector with the spatially resolved field in the scatterer domain  $\mathbb{N}$ . This formulation of the scattering problem has an advantage over a standard site-by-site transfer matrix method in that the scatterer can be of arbitrary type: Keeping a two-terminal geometry, the scatterer may contain, e. g., side-coupled sites or a 2D cluster of interconnected sites. No explicit single-node transfer matrices propagating the wave along the scatterer need to be specified, rather the complete Hamiltonian under appropriate indexing is utilized directly.

## Appendix B: Derivation of general mapping relation and current connection

The NLCs  $q_{n,S}^\pm$  and their alternatives  $\hat{q}_{n,S}^\pm$  for a general state  $|\psi\rangle$  can be expressed together via a matrix product acting on



- [29] P. A. Kalozoumis, C. V. Morfonios, F. K. Diakonou, and P. Schmelcher, “ $\mathcal{PT}$ -symmetry breaking in waveguides with competing loss-gain pairs,” *Phys. Rev. A* **93**, 063831 (2016).
- [30] P. A. Kalozoumis, O. Richoux, F. K. Diakonou, G. Theocharis, and P. Schmelcher, “Invariant currents in lossy acoustic waveguides with complete local symmetry,” *Phys. Rev. B* **92**, 014303 (2015).
- [31] B. Bagchi, C. Quesne, and M. Znojil, “Generalized continuity equation and modified normalization in  $\mathcal{PT}$ -symmetric quantum mechanics,” *Mod. Phys. Lett. A* **16**, 2047 (2001).
- [32] G. S. Japaridze, “Space of state vectors in  $\mathcal{PT}$ -symmetric quantum mechanics,” *J. Phys. A: Math. Gen.* **35**, 1709 (2002).
- [33] L. P. Withers Jr. and F. A. Narducci, “A bilocal picture of quantum mechanics,” *J. Phys. A: Math. Theor.* **48**, 155304 (2015).
- [34] H. Schomerus, “From scattering theory to complex wave dynamics in non-Hermitian  $\mathcal{PT}$ -symmetric resonators,” *Phil. Trans. R. Soc. A* **371**, 20120194 (2013).
- [35] D. Sinha and P. K. Ghosh, “Symmetries and exact solutions of a class of nonlocal nonlinear schrödinger equations with self-induced parity-time-symmetric potential,” *Phys. Rev. E* **91**, 042908 (2015).
- [36] C. M. Bender and S. Boettcher, “Real spectra in Non-Hermitian Hamiltonians having  $\mathcal{PT}$  symmetry,” *Phys. Rev. Lett.* **80**, 5243 (1998).
- [37] S. Weigert, “The physical interpretation of  $\mathcal{PT}$ -invariant Potentials,” *Czech. J. Phys.* **54**, 1139 (2004).
- [38] F. Cannata, J.-P. Dedonder, and A. Ventura, “Scattering in -symmetric quantum mechanics,” *Ann. Phys.* **322**, 397 (2007).
- [39] Y. D. Chong, L. Ge, and A. D. Stone, “ $\mathcal{PT}$ -Symmetry breaking and Laser-Absorber modes in optical scattering systems,” *Phys. Rev. Lett.* **106**, 093902 (2011).
- [40] P. Ambichl, K. G. Makris, L. Ge, Y. Chong, A. D. Stone, and S. Rotter, “Breaking of  $\mathcal{PT}$  symmetry in bounded and unbounded scattering systems,” *Phys. Rev. X* **3**, 041030 (2013).
- [41] S. Garmon, M. Gianfreda, and N. Hatano, “Bound states, scattering states, and resonant states in  $\mathcal{PT}$ -symmetric open quantum systems,” *Phys. Rev. A* **92**, 022125 (2015).
- [42] S. Longhi, “Non-Hermitian tight-binding network engineering,” *Phys. Rev. A* **93**, 022102 (2016).
- [43] H. S. Eisenberg, Y. Silberberg, R. Morandotti, and J. S. Aitchison, “Diffraction management,” *Phys. Rev. Lett.* **85**, 1863 (2000).
- [44] M. H. Teimourpour, R. El-Ganainy, A. Eisfeld, A. Szameit, and D. N. Christodoulides, “Light transport in  $\mathcal{PT}$ -invariant photonic structures with hidden symmetries,” *Phys. Rev. A* **90**, 053817 (2014).
- [45] N. Bender, H. Li, F. M. Ellis, and T. Kottos, “Wave-packet self-imaging and giant recombinations via stable Bloch-Zener oscillations in photonic lattices with local  $\mathcal{PT}$  symmetry,” *Phys. Rev. A* **92**, 041803 (2015).
- [46] M. Wimmer, A. Regensburger, M.-A. Miri, C. Bersch, D. N. Christodoulides, and U. Peschel, “Observation of optical solitons in  $\mathcal{PT}$ -symmetric lattices,” *Nat. Comm.* **6**, 7782 (2015).
- [47] H. U. Baranger, D. P. DiVincenzo, R. A. Jalabert, and A. D. Stone, “Classical and quantum ballistic-transport anomalies in microjunctions,” *Phys. Rev. B* **44**, 10637 (1991).
- [48] T. B. Boykin, M. Luisier, and G. Klimeck, “Current density and continuity in discretized models,” *Eur. J. Phys.* **31**, 1077 (2010).
- [49] A. Szameit, F. Dreisow, T. Pertsch, S. Nolte, and A. Tünnermann, “Control of directional evanescent coupling in fs laser written waveguides,” *Opt. Express* **15**, 1579 (2007).
- [50] F. Haake, “Time reversal and unitary symmetries,” in *Quantum Signatures of Chaos* (Springer Berlin Heidelberg, 2001), pp. 15.
- [51] M. Golshani, S. Weimann, Kh. Jafari, M. K. Nezhad, A. Langari, A. R. Bahrampour, T. Eichelkraut, S. M. Mahdavi, and A. Szameit, “Impact of loss on the wave dynamics in photonic waveguide lattices,” *Phys. Rev. Lett.* **113**, 123903 (2014).
- [52] A. K. Sarma, M.-A. Miri, Z. H. Musslimani, and D. N. Christodoulides, “Continuous and discrete schrödinger systems with parity-time-symmetric nonlinearities,” *Phys. Rev. E* **89**, 052918 (2014).
- [53] W. G. Kelley and A. C. Peterson, *Difference Equations: An Introduction with Applications* (Academic Press, San Diego, 2000).
- [54] S. Klaiman and L. S. Cederbaum, “Non-Hermitian Hamiltonians with space-time symmetry,” *Phys. Rev. A* **78**, 062113 (2008).
- [55] B. Zhu, R. Lü, and S. Chen, “ $\mathcal{PT}$  symmetry in the non-Hermitian Su-Schrieffer-Heeger model with complex boundary potentials,” *Phys. Rev. A* **89**, 062102 (2014).
- [56] A. K. Harter, T. E. Lee, and Y. N. Joglekar, “ $\mathcal{PT}$ -breaking threshold in spatially asymmetric Aubry-André and Harper models: Hidden symmetry and topological states,” *Phys. Rev. A* **93**, 062101 (2016).
- [57] T. Wulf, C. V. Morfonios, F. K. Diakonou, and P. Schmelcher, “Exposing local symmetries in distorted driven lattices via time-averaged invariants,” *Phys. Rev. E* **93**, 052215 (2016).
- [58] A. Szameit, I. L. Garanovich, M. Heinrich, A. A. Sukhorukov, F. Dreisow, T. Pertsch, S. Nolte, A. Tünnermann, and Y. S. Kivshar, “Observation of Defect-Free surface modes in optical waveguide arrays,” *Phys. Rev. Lett.* **101**, 203902 (2008).
- [59] I. L. Garanovich, S. Longhi, A. A. Sukhorukov, and Y. S. Kivshar, “Light propagation and localization in modulated photonic lattices and waveguides,” *Phys. Rep.* **518**, 1 (2012).
- [60] S. Longhi, “Transmission and localization control by ac fields in tight-binding lattices with an impurity,” *Phys. Rev. B* **73**, 193305 (2006).
- [61] M. Grifoni and P. Hänggi, “Driven quantum tunneling,” *Phys. Rep.* **304**, 229 (1998).
- [62] S. Longhi and G. D. Valle, “Floquet bound states in the continuum,” *Sci. Rep.* **3**, 2219 (2013).
- [63] E. H. Lieb and D. C. Mattis, *Mathematical physics in one dimension: exactly soluble models of interacting particles* (Academic Press, 1966).
- [64] L. Ge, Y. D. Chong, and A. D. Stone, “Conservation relations and anisotropic transmission resonances in one-dimensional  $\mathcal{PT}$ -symmetric photonic heterostructures,” *Phys. Rev. A* **85**, 023802 (2012).
- [65] A. E. Miroschnichenko, S. F. Mingaleev, S. Flach, and Y. S. Kivshar, “Nonlinear fano resonance and bistable wave transmission,” *Phys. Rev. E* **71**, 036626 (2005).
- [66] N. Boechler, J. Yang, G. Theocharis, P. G. Kevrekidis, and C. Daraio, “Tunable vibrational band gaps in one-dimensional diatomic granular crystals with three-particle unit cells,” *J. Appl. Phys.* **109**, 074906 (2011).
- [67] M. Röntgen *et al.*, in preparation.
- [68] J. Stockhofe and P. Schmelcher, “Sub- and supercritical defect scattering in schrödinger chains with higher-order hopping,” *Phys. Rev. A* **92**, 023605 (2015).
- [69] J. Stockhofe and P. Schmelcher, “Bloch dynamics in lattices with long-range hopping,” *Phys. Rev. A* **91**, 023606 (2015).